Contribution of YjbIH to virulence factor expression and host colonization in *Staphylococcus aureus*

Crystal M. Austin[a], Siamak Garabaglu[b], Christina N. Krute[a], Miranda J. Ridder[a], Nichole A. Seawell[a], Mary A. Markiewicz[a], Jeffrey M. Boyd[b], Jeffrey L. Bose[a#]

[a]University of Kansas Medical Center, Department of Microbiology, Molecular Genetics and Immunology, Kansas City, KS, 66061

[b]Rutgers University, Department of Biochemistry and Microbiology, New Brunswick, NJ 08901

Running title: YjbIH contributes to *S. aureus* virulence

[#]Address correspondence to Dr. Jeffrey Bose, jbose@kumc.edu

Keywords: YjbH, YjbI, staphyloxanthin, aureolysin, Spx, *Staphylococcus aureus*

ABSTRACT

To persist within the host and cause disease, *Staphylococcus aureus* relies on its ability to precisely fine-tune virulence factor expression in response to rapidly-changing environments. During an unbiased transposon mutant screen, we observed that disruption of the two-gene operon, *yjbIH*, resulted in decreased pigmentation and aureolysin activity relative to the wild-type strain. Further analyses revealed that YjbH, a predicted thioredoxin-like oxidoreductase, is mostly responsible for the observed *yjbIH* mutant phenotypes, though a minor role exists for the putative truncated hemoglobin YjbI. These differences were due to significantly decreased expression of *crtOPQMN* and *aur*. Previous studies found that YjbH targets the disulfide- and oxidative-stress responsive regulator Spx for degradation by ClpXP. The absence of *yjbH* or *yjbI* resulted in altered sensitivities to nitrosative and oxidative stress and iron deprivation. Additionally, aconitase activity was altered in the *yjbH* and *yjbI* mutant strains. Decreased pigmentation and Aur activity in the *yjbH* mutant was found to be Spx-dependent. Lastly, we used a murine sepsis model to determine the effect of the *yjbIH* deletion on pathogenesis and found that the mutant was better able to colonize the kidneys and spleens during an acute infection than the wild-type strain. These studies identify changes in pigmentation and protease activity in response to YjbIH and are the first to show a role for these proteins during infection.

INTRODUCTION

Staphylococcus aureus is a highly versatile pathogen capable of causing disease in nearly every bodily tissue ranging from mild skin and wound infections to more severe

infections, including osteomyelitis, endocarditis, pneumonia, and sepsis (1-4). Its ability to adapt to a variety of anatomical niches is largely attributed to its complex, yet precise modulation of virulence factor expression in response to environmental and temporal fluxes (5, 6). The major US-dominating strain of community-associated methicillin resistant *Staphylococcus aureus* (CA-MRSA) known as USA300 has enhanced virulence properties due to altered expression of genome-encoded virulence factors, such as phenol soluble modulins and α-toxin (7-10). A better understanding of how this strain orchestrates virulence factor production may lead to fresh perspectives on MRSA pathogenesis.

To cause disease, *S. aureus* must survive the multi-component attack of the immune system. Initially, this includes innate immune system factors such as complement, antimicrobial peptides, and oxidative and nitrosative stress. To aid its defense, *S. aureus* is equipped with a battery of virulence factors, including 10 major extracellular proteases that target host immune components, regulate the abundance and stability of other secreted and surface-associated virulence factors, and are involved in nutrient acquisition (11-21). Aureolysin (Aur) is a zinc-metalloprotease that sits atop a protease activation cascade and is responsible for activating the SspA (V8) serine and SspB cysteine proteases (22, 23). These proteases have been shown to inactivate complement and cleave immunoglobins (14, 21, 24). Additionally, Aur has been shown to regulate the levels and stabilities of 83% (225 proteins) of all SaeRS-regulated proteins (25). Transcription of *aur* is positively regulated by the global activator, MgrA, and the quorum sensing protein, AgrA, in combination with the small RNA, RNAIII (26). *aur* is negatively regulated by the DNA-binding protein, SarA, and

66 Rot, the repressor of toxins (26, 27). Adding complexity to this regulation, SarA activity
67 is positively regulated by the alternative sigma factor, σ^B, among other transcription
68 factors (28, 29). Lastly, Aur is negatively regulated at the post-transcriptional level by
69 the two-component system, SaeRS (30).

70 To combat oxidative and nitrosative stress during host colonization, *S. aureus* is
71 well-equipped with a variety of resistance mechanisms and detoxification proteins. In
72 addition, staphyloxanthin, the pigment that gives *S. aureus* its characteristic golden
73 color, has multiple functions, including serving as an antioxidant. Its ability to quench
74 singlet oxygen affords the bacterium protection against toxic reactive oxygen species
75 (ROS) (31, 32). Studies have demonstrated that strains lacking pigmentation are more
76 susceptible to killing by neutrophils, which attack bacterial cells with the release of ROS
77 and reactive nitrogen species (RNS) (33-35). Pigment-deficient strains are attenuated
78 for virulence in a subcutaneous abscess model (33). Biosynthesis of staphyloxanthin is
79 accomplished via five proteins encoded by the *crtOPQMN* operon, transcription of which
80 is positively regulated by σ^B and the AirSR two-component system (36, 37). It is
81 negatively regulated by the small RNA, SsrA (38).

82 In addition to pigment, *S. aureus* possesses numerous oxidative and nitrosative
83 stress defense proteins. To combat nitric oxide ($NO^{\cdot}$) stress, this bacterium is equipped
84 with Hmp, a $NO^{\cdot}$-detoxifying flavohemoglobin (39, 40). It has two superoxide
85 dismutases, SodA and SodM, which catalyze the breakdown of O_2^- (41, 42), the H_2O_2-
86 degrading proteins catalase (KatA), and alkyl hydroperoxide reductase (AhpC) (43, 44).
87 One consequence of oxidative stress is the formation of disulfide bonds between
88 cysteine residues, resulting in protein inactivation. To maintain a reduced cytoplasm,

bacteria rely on the redox cycling reactions of thioredoxin (TrxA) and thioredoxin reductase (TrxB), which are both essential proteins in *S. aureus* (45-47). Furthermore, *S. aureus* has three paralogs of the methionine sulfoxide reductase A protein (MsrA) and one MsrB protein, which are known to repair oxidized forms of methionine residues (48, 49).

During a screen of the Nebraska Transposon Library (50), we observed that disruption of the *yjbIH* operon resulted in decreased pigmentation and Aur activity. Both genes are annotated as hypothetical proteins, though structural prediction analysis demonstrates that YjbI is a truncated hemoglobin (trHb) and YjbH is a thioredoxin-like thiol/disulfide oxidoreductase (51). Studies in *Bacillus subtilis* and limited studies in *S. aureus* have demonstrated YjbH to be an adaptor protein for Spx, a transcriptional regulator that controls expression of numerous genes, including *trxA* and *trxB*, in response to disulfide and oxidative stress (52-56). In this study, we sought to characterize the *S. aureus yjbIH* mutant phenotypes and understand the mechanism by which these proteins alter staphyloxanthin production and Aur expression. The data collected by our group are aligned with a model for Spx-dependent regulation of *crtOPQMN* and *aur*, and we revealed a role for σ^B in our mutant strain phenotypes. Interestingly, we found that the *yjbIH* mutant strain is more virulent than the wild-type strain in a murine sepsis infection. We predict that YjbH is influencing the activity of both Spx and and/or another regulatory protein(s), perhaps σ^B, such that expression and activity of key virulence factors is altered.

MATERIALS AND METHODS

Bacterial strains and growth conditions. For all experiments, *S. aureus* strains (Table 1) were cultured from -80°C freezer stocks on tryptic soy agar (TSA) and sub-cultured overnight in tryptic soy broth (TSB) supplemented with chloramphenicol (10 μg ml^{-1}), erythromycin (2 - 5 μg ml^{-1}), trimethoprim (10 μg ml^{-1}), kanamycin (100 μg ml^{-1}), or tetracycline (1 μg ml^{-1}) when necessary. *Escherichia coli* DH5α (57) and DH5α-λ*pir* (58) were used for cloning and grown in LB (lysogeny broth) medium supplemented with ampicillin (100 μg ml^{-1}) or trimethoprim (10 μg ml^{-1}).

Construction and complementation of mutant strains. Plasmids to generate deletion strains JLB110, JLB134, and JLB147 (Table 1) were constructed using AH1263 genomic DNA and KOD DNA Polymerase (Novagen). For JLB110, primers JBKU19 and JBKU20 were used to amplify a 717-bp fragment upstream of *yjbI*, and JBKU23 and JBKU24 were used to amplify a 730-bp fragment downstream of *yjbH*. Both fragments were simultaneously cloned into the temperature sensitive, allelic exchange plasmid pJB38 (59) using KpnI and SalI to generate pJB1021. For JLB134, primers JBKU19 and JBKU20 were used to amplify a 717-bp fragment upstream of *yjbI* containing the *yjbI* promoter, and JBKU43 and JBKU44 were used to amplify a 690-bp fragment downstream of *yjbI* that were simultaneously cloned into pJB38 using KpnI and SalI to create pCP1. For JLB147, JBKU23 and JBKU24 primers were used to amplify a 730-bp fragment downstream of *yjbH* that was cloned into pJB38 using SmaI to create pCP2. Then, primers CP1 and JBKU42 were used to amplify an 839-bp region upstream of *yjbH* containing the entire *yjbI* gene along with its promoter and cloned into pCP2 using KpnI and NheI to generate pCP3. All plasmid constructions were performed in *E. coli*.

The plasmids were then transformed into RN4220 (60) and transduced into AH1263 using ϕ11 as previously performed (61). Finally, allelic exchange (62) was performed and the mutant was verified via PCR following DNA isolation as previously described (63). Transposon insertions of *sigB*, *crtM*, *clpP*, and *hmp* (50) were transferred to either AH1263 or JLB110 strains by transduction of chromosomal alleles via ϕ11 resulting in JLB143, JLB179, JLB176, JLB178, and JLB146. JLB126 was constructed via allelic exchange using pKAN (59) to replace the Erm cassette in NE1109 with a Kan cassette. Then, the *sigB*::*kan*^{R} mutation was transferred to AH1263 and JLB110 via ϕ11-mediated transduction, resulting in JLB174 and JLB175, respectively. For generation of *spx* mutants, the plasmid pMK4-pGlyS-*trxA* (64) was first transformed into RN4220 and then transferred to AH1263 via transduction with ϕ11. ϕ85 was used to transfer the *spx*::*kan*^{R} mutation from CB1400 (64) into AH1263 pMK4-pGlyS-*trxA*, thereby generating JLB248. The NE1800 transposon insertion was then transferred to JLB248 via transduction with ϕ11, resulting in JLB249. JLB247 was constructed via ϕ85-mediated transduction of the *geh*::pCL25 *spx*$^+$ *tet*^{R} fragment from CB1400 into JLB110. ϕ11 was then propagated using JLB247 as the donor strain and was used to transduce the *geh*::pCL25 *spx*$^+$ *tet*^{R} fragment into JLB249, resulting in JLB250. JLB264 was constructed via allelic exchange of JLB130 and pTET. JLB277 and JLB280 were generated via ϕ11-mediated transduction of the *sigB*::*tet* fragment from JLB264 into JLB248 and JLB249, respectively.

The *yjbIH* (JLB110), *yjbI* (JLB134), and *yjbH* (JLB147) mutant strains were complemented using pKK22 as the base plasmid (65). Primers JBPR01 and CP2 were used to amplify a 1.7-kb fragment containing the wild-type *yjbIH* operon and cloned into

158 pKK22 using BamHI and NheI to generate pCP4. The *yjbH* complement plasmid, pCP5,
159 was generated by amplifying a 1.4-kb fragment containing the *yjbH* gene along with its
160 native promoter using JBPR01 and CP7 from JLB134 genomic DNA and was then
161 cloned into the BamHI and AvrII sites of pKK22. Primers CP3 and CP8 were used to
162 amplify a 1.6-kb fragment containing the *yjbI* gene from pCP3 and was then cloned into
163 the BamHI and AvrII sites of pKK22, resulting in pCP6. Each of the complement
164 plasmids (pCP4, pCP5, and pCP6) were transformed into *E. coli* DH5αλ*pir*, then
165 transformed into RN4220, and finally transduced into mutant strains using ϕ11. An
166 additional complement plasmid was made and used in Fig S1. pJB158 was generated
167 by amplifying the *yjbIH* operon and upstream sequence from AH1263 (primers JBPR01
168 and JBPR02) and ligating into pCM28 digested with BamHI and PstI. All plasmids were
169 verified via sequencing by ACGT, Inc.
170
171 **Carotenoid pigment assay.** The method used to extract and to quantify pigment
172 production among strains was modified from Morikawa, K., et al. and Sapp, A.M. et al.
173 (66, 67). Overnight cultures were standardized to OD_{600} = 1.0 and 40 µl spots were
174 pipetted onto TSA in triplicate. After overnight incubation, cells were scraped from the
175 surface and resuspended in 1 ml H_2O. 20 µl was removed to determine OD_{600}, and the
176 remaining suspension was centrifuged at 21,130 x *g* for 3 min. The supernatant was
177 decanted and the pellet resuspended in 420 µl MeOH, vortexed for 10 sec, and
178 incubated at 55°C for 5 min. The suspension was then centrifuged at 21,130 x *g* for 2
179 min, and 350 µl of the supernatant was added to a cuvette containing 650 µl MeOH.
180 Absorbance at 465 nm was recorded, and the amount of pigment produced among

strains was normalized by dividing the A_{465} by the relative OD_{600} (which was calculated by dividing the individual OD_{600} by the average OD_{600} of the AH1263 wild-type strain). For figure panels depicting colony pigment colors, overnight cultures were resuspended to OD_{600} = 1.0 in 1 ml of TSB, and 1 µl spots were pipetted onto TSA and incubated overnight at 37°C.

Construction of promoter-*lacZ* fusions and β-galactosidase assays. To conduct activity assays for the *crtOPQMN* and *aur* promoters, we constructed *lacZ*-reporter plasmids pCP7 and pCK3, respectively. For pCP7, primers CP9 and CP10 were used to amplify a 224-bp fragment containing the *crtOPQMN* promoter and cloned into pJB185 (68) using EcoRI and XbaI. For pCK3 generation, primers CNK11 and CNK12 were used to amplify a 483-bp fragment containing the *aur* promoter sequence, which was cloned into pJB185 using EcoRI and XbaI. β-galactosidase activities were calculated using a method described by Lehman M.K., et al. (69). Overnight cultures were diluted to OD_{600} = 0.1 in 12.5 ml of TSB in 125-ml flasks. At each time point, 1 ml was harvested, centrifuged at 21,130 x *g* for 1 min, and then resuspended in 1.2 ml of Z-buffer. The cell suspension was subjected to lysis using the FastPrep-24 5G homogenizer (MP Biomedicals) using 0.1 mm glass beads and the manufacturer's setting for *S. aureus*. Cellular debris was pelleted by centrifugation at 21,130 x *g* for 5 min, and the lysate was transferred to a new tube. A sample of lysate was removed (50 – 200 µl) and combined with Z-buffer for a total volume of 700 µl to which 140 µl of *o*-nitrophenyl β-D-galactopyranoside (ONPG) (4 mg ml^{-1} (w/v, in 40 mM NaH_2PO_4, 60 mM Na_2HPO_4, pH 7.0)) was added and incubated statically at 37°C until the sample turned

204 slightly yellow. At this point, 200 µl of 1 M $NaCO_3$ was added to stop the reaction, and
205 the samples were then centrifuged at 21,130 x *g* for 30 sec to remove any remaining
206 cellular debris. The sample was transferred to a cuvette and absorbance read at 420
207 nm. Bradford assays were performed by using the Protein Assay Dye Reagent (Bio-
208 Rad, Hercules, CA). Modified Miller units were calculated using protein concentration
209 and is reported on a per mg protein basis.
210
211 **Protease assays.** As described in (70), overnight cultures were resuspended to
212 OD_{600} = 1.0 in 1 ml of TSB, and 1 µl spots were pipetted onto 1.0% skim milk agar
213 plates and incubated for 48 hours at 37°C. Images were taken using an ImageQuant
214 LAS-4000 Imaging System (Fujifilm). All images in a single figure panel were taken
215 under the same camera settings and adjusted equally.
216
217 **RNA isolation, cDNA synthesis, and qPCR.** Overnight cultures were
218 resuspended to OD_{600} = 0.1 in 25 ml of TSB in a 250-ml flask and allowed to incubate at
219 37°C with shaking at 250 RPM. 3 ml of culture was then transferred to a conical tube
220 containing 5 ml of cold PBS and centrifuged at 4,500 x *g* for 5 min at 4°C. The
221 supernatant was removed and the pellet frozen at -80°C. After thawing on ice, the pellet
222 was resuspended in TE buffer and transferred to a Lysing Matrix B Tube (MP
223 Biomedicals), and cells were subjected to lysis using the FastPrep-24 5G homogenizer
224 (MP Biomedicals). Total RNA was extracted using the RNeasy Mini Kit (Qiagen) and
225 treated with DNase (TURBO DNA-*free* Kit (Invitrogen)). RNA was quantified using a
226 NanoDrop One (ThermoFisher Scientific) and quality was assessed using an Agilent

TapeStation 4200 (KUMC Genome Sequencing Facility). cDNA was synthesized using the QuantiTect Reverse Transcription Kit (Qiagen) with 500 ng of total RNA used as the template. The cDNA was diluted 50-fold in nuclease-free H_2O and aliquoted into 1.5-ml tubes. A reaction mixture containing FastStart Essential DNA Green Master (Roche), primers (5 μM each), and H_2O was added to the diluted cDNA. Finally, 19 μL of this mixture was aliquoted in triplicate into a 96-well plate and amplification was performed in a LightCycler96 (Roche). Relative transcript abundances were calculated using the comparative threshold cycle (C_T) method (71) and the value of each target gene was normalized to the housekeeping sigma factor, *sigA* (*rpoD*) (72, 73). Fold-change expression was calculated relative to the wild-type strain.

RT-PCR. RNA was isolated from cells grown for 7 h as described above for qPCR. cDNA was synthesized using the QuantiTect Reverse Transcription Kit (Qiagen) with 500 ng of total RNA with a 45-minute synthesis step. Reactions were carried out with non-specific primers both with and without (negative control) reverse transcriptase enzyme.

$NO^{\cdot}$ sensitivity assays. Nitrosative stress assays were performed as previously described (74) with some modifications. Cells were grown overnight in TSB, transferred to a conical tube, and centrifuged at 3,157 x *g* for 5 min. The pellet was washed twice with PBS and resuspended in LB with 0.5% glucose and 0.05 M Tris, pH 7.4 (LBGT) medium. Cultures were resuspended to OD_{600} = 0.01 and 100 μl was added to a 96-well plate in triplicate. The $NO^{\cdot}$ donor, diethylenetraimine NONOate (DETA-NO; Cayman

Chemical) was added to the wells at a final concentration of 10 mM. LBGT was used to bring the total volume in the well up to 200 µl and growth was monitored using a Tecan Spark 10M Multimode Microplate Reader and incubated for 16 h at 37°C with orbital shaking at 510 RPM.

H_2O_2 killing assays. H_2O_2 assays were conducted as previously described (75). Briefly, overnight TSB cultures were pelleted and then resuspended in PBS to OD_{600} = 0.7 in 1 ml. Cell suspensions were then treated with or without 1 M H_2O_2 for one hour. Subsequently, 50 µl of treated samples were diluted 1:20 in PBS containing catalase (1,300 units ml^{-1}), gently mixed, and incubated for 5 min. Five µl of the final dilutions ranging from 10^{-1} to 10^{-6} were plated on TSA and assessed for cell survival.

Methyl viologen and 2,2-dipyridyl sensitivity assays. For methyl viologen assays, overnight TSB cultures were serially diluted and five µl aliquots were individually spot plated onto TSA medium containing 25 mM methyl viologen or 1mM 2,2-dipryidyl (DIP).

Aconitase assays. Overnight TSB cultures were diluted 1:100 in TSB or TSB with chloramphenicol. Cells were grown in 10 ml-culture tubes containing either 1 ml (high-aeration) or 5 ml (low-aeration) of medium as previously described (76). After 12 hours of culture, 1 ml of cells were pelleted, washed with PBS, and stored at -80°C until use. AcnA activity was determined as previously described (77).

Diamide assays. As described previously (64, 78), cultures were grown overnight in TSB and resuspended to OD_{600} = 0.2. Serial dilutions from 10^{-1} to 10^{-4} were made and 1 μl spots were plated onto TSA containing 0.2 mM diamide (Sigma). Plates were incubated overnight at 37°C.

Mouse infection assays. These studies were conducted in strict accordance with the recommendations in the *Guide for the Care and Use of Laboratory Animals* of the National Institutes of Health (79). The Institutional Animal Care and Use Committee (IACUC) of the University of Kansas Medical Center approved this protocol. 8-week-old C57BL/6J female mice (Jackson Laboratories) were infected retro-orbitally with either a low-dose ($4x10^6$ CFU) or high dose (~$1x10^7$ CFU) of bacteria. Mice weights were recorded every other day and fitness scores were assigned. After 5 or 6 days, the mice were humanely euthanized and kidney, liver, and spleens were harvested. Kidneys and spleens were homogenized using lysing matrix H tubes. Livers were divided in half and homogenized using lysing matrix I tubes (MP Biomedicals) with subsequent pooling of the two homogenates. Organs were subjected to lysis in PBS using the FastPrep-24 5G instrument (MP Biomedicals) according to manufacturer's recommendations. Homogenates were serially diluted in PBS + 0.1% Triton X-100 and plated onto TSA. Colonies were counted after overnight incubation.

Statistical analysis. All statistical analyses were performed using Prism, version 6 (GraphPad). Statistical significance was determined using unpaired *t*-test, one-way or

two-way ANOVA, as indicated. $p < 0.05$ was considered statistically significant unless otherwise stated.

RESULTS

Pigment and aureolysin activity are decreased in *yjbIH* and *yjbH* mutants. During a screen of the Nebraska Transposon Mutant Library (50), we found that disruption of the two-gene operon, *yjbIH* (SAUSA300_0904-0903), resulted in decreased production of staphyloxanthin, the yellowish-orange pigment characteristic of *S. aureus*, and decreased protease activity associated with the zinc metalloprotease, aureolysin (Aur) (Fig. S1A). Returning the *yjbIH* genes to either mutant strain via a plasmid reversed the phenotypic effects of the insertions. The transcription of *yjbI* and *yjbH* as a single transcript was verified by RT-PCR (Fig. S1B).

The insertion of a transposon results in polar effects on downstream genes; therefore, to determine if these phenotypes were due to polar effects, we created strains with individual in-frame gene deletions and a strain with a double gene deletion. Growth analysis of the mutants revealed that the *yjbIH* and *yjbH* mutants were reproducibly slightly delayed in initial growth but reached wild-type levels by 3 h, at which point all strains grew similarly (Fig. S2). During routine culturing, it was noted that the *yjbH* mutant strain was similar in color to the *yjbIH* mutant. To determine pigment differences, we quantified carotenoid pigment and found that the *yjbH* mutant produced significantly less pigment than the wild-type strain. The *yjbIH* and *yjbH* mutants were not devoid of pigment as they produced more than the *crtM* mutant control (Fig. 1A). By contrast, the *yjbI* mutant resembled the wild-type strain.

As stated above, we found that activity of the extracellular protease, aureolysin, was decreased in the *yjbI* and *yjbH* transposon mutants. We cultured the wild-type, *yjbI*, *yjbH*, and *yjbIH* deletion strains along with the complement strains on 1.0% skim milk agar. An *aur* mutant was included as a negative control. As shown in Figure 1B, we observed that the *yjbIH* and *yjbH* mutant strains had decreased Aur activity in comparison to the wild-type strain. Minimal difference was observed in the *yjbI* mutant. Together, these data demonstrated that YjbH was the major contributor to the pigmentation and Aur activity phenotypes observed in the original transposon mutants.

YjbI and YjbH affect transcription of *crtOPQMN* and *aur*. To test whether the YjbH-dependent pigment and Aur phenotypes were due to altered expression of *crtOPQMN* and *aur*, we constructed β-galactosidase reporter plasmids containing *lacZ* under the transcriptional control of the *crtOPQMN* or *aur* promoters. In contrast to the wild-type strain, where transcription of the *crtOPQMN* promoter gradually increased throughout the growth cycle, we observed that the *yjbIH* strain had a significant reduction in *crtOPQMN* promoter activity at each time point tested (Fig. 2A). Expression was restored when *yjbIH* was provided on a plasmid. We observed no expression in a *sigB* mutant, the known crucial activator of the *crtOPQMN* promoter. To delineate the individual contributions of YjbI and YjbH to changes in *crtOPQMN* expression, we analyzed promoter activity in the individual mutants and their respective complement strains (Fig. 2C). Notably, we observed that both YjbI and YjbH contribute to the decreased transcription of *crtOPQMN* when tested in broth culture, despite no observed difference in pigmentation on plates in the *yjbI* mutant.

β-galactosidase assays with a P_{aur}-*lacZ* transcriptional fusion revealed that in wild-type cells, *aur* promoter activity increased throughout the growth cycle and peaks at 4h (Fig. 2B). A similar trend was seen for the *yjbIH* mutant, but *aur* expression was decreased by at least two-fold at each time point. This defect could be complemented by returning the wild-type copy of *yjbIH* via a plasmid. A *sigB* mutant was again used here as a control as σ^B is known to repress *aur* expression. To determine the individual contribution of YjbI and YjbH to the *yjbIH* mutant phenotype, we monitored promoter activity at the late exponential phase of growth (Fig. 2D). We found that the absence of *yjbH* resulted in a phenotype similar to the *yjbIH* mutant with approximately two-fold less *aur* expression as compared to the wild-type strain. While the *yjbI* mutant consistently showed a modest decrease, it was not statistically significant.

The *yjbIH* mutants have altered sensitivities to nitrosative and oxidative stress. Previous studies have shown that truncated hemoglobins are involved in O_2-sensing and the detoxification of nitric oxide ($NO\cdot$), and YjbH has been shown to control the abundance of Spx, a transcriptional regulator that responds to oxidative stress (78, 80-82). In addition, thioredoxins are known to help maintain a reduced cytoplasm and contribute to the defense against oxidative stress. Moreover, a recent transposon sequencing (Tn-Seq) experiment identified YjbH as being required for resistance to $NO^{\cdot}$ (83). We therefore tested the sensitivities of *yjbI* and *yjbH* mutants to nitrosative and oxidative stressors. For nitrosative stress, we exposed cells to the $NO^{\cdot}$ donor, DETA-NO, at the time of inoculation and compared growth of the strains as in previous studies (74, 83). Treatment with DETA-NO had the largest impact on the *yjbIH* strain and an

364 intermediate effect on the *yjbH* strain as compared to the wild-type (Fig. 3A). The *yjbI*
365 strain displayed a similar phenotype to the wild-type strain, though we consistently
366 observed that this mutant grew slightly better. A mutant deficient in the NO·-
367 detoxification protein, Hmp, was included as a control. To conduct statistical analyses,
368 the area under the curves for the NO·-treated samples were determined for hours 7.5 to
369 14. As seen in Figure 3B, both the *yjbIH* and *yjbH* mutants showed statistically-poorer
370 growth under $NO^{\cdot}$ stress. Furthermore, we tested the susceptibility of the transposon
371 mutants for *yjbI* and *yjbH* (Fig. S3) to verify our deletion strain phenotypes. Indeed, we
372 found that both transposon mutants were more sensitive to treatment with DETA-NO as
373 compared to the JE2 wild-type strain. These data confirm the previous report (83)
374 identifying that YjbH is important for resistance to $NO^{\cdot}$ stress.

375 We examined the sensitivities of the strains to H_2O_2 and to methyl viologen, a
376 superoxide generator (O_2^{-}). As seen in Figure 4, the *yjbH* and *yjbIH* strains were more
377 susceptible to killing by H_2O_2 whereas the *yjbI* mutant behaved similar to the wild-type
378 strain. By contrast, all of the mutant strains displayed increased resistance to methyl
379 viologen when compared to the wild-type strain (Fig. 4C). Taken together, it appeared
380 that YjbH and YjbI sensitized the cell to superoxide, and YjbH was important for H_2O_2
381 resistance.

382 We sought to determine if this altered resistance was due to transcriptional
383 effects on genes known to encode proteins involved in ROS/RNS resistance. To this
384 end, qRT-PCR was performed on RNA isolated from wild-type and *yjbIH* strains grown
385 to late exponential phase. All of the observed transcriptional changes in the *yjbIH* strain
386 were modest (<2.5-fold higher in *yjbIH* mutant) and only catalase (*katA*), alkyl

hydroperoxide reductase (*ahpC*), superoxide dismutase (*sodA* and *sodM*), and *trxB* reached statistical significance (Fig. S4). Collectively, the results suggested that the *yjbIH* mutant had altered sensitivities to oxidative and nitrosative stress and modest alterations in transcription of ROS/RNS defense genes.

The *yjbIH* mutants have decreased aconitase activity and increased sensitivity to iron chelation. *S. aureus* contains a single aconitase protein (AcnA) which requires an [4Fe-4S] cluster for activity (84). The iron-sulfur cluster is highly susceptible to disassembly by ROS, rendering the protein inactive (85). *S. aureus* strains lacking superoxide dismutase or catalase have decreased AcnA activity when cultured with high aeration (86, 87). We hypothesized that since the *yjbI*, *yjbH*, and *yjbIH* mutants have varying sensitivities to ROS, they may have altered cellular ROS, which would lead to changes in aconitase activity. To test this, we assessed aconitase activity in the wild-type and mutant strains under high and low aeration (Fig. 5A & B). Under high aeration, all three mutant strains had less aconitase activity than the wild-type strain, indicating roles for both YjbH and YjbI in AcnA activity. By contrast, under low aeration, only the *yjbH* and *yjbIH* mutants had decreased activity.

It was possible that *yjbIH* mutants have altered *acnA* transcription; therefore, we generated *acnA* knockouts in wild-type and *yjbIH* mutant strains and expressed *acnA* from a non-native promoter. Upon induction of *acnA* transcription (Fig. 5C), there was a significant decrease in AcnA activity in the *yjbI*, *yjbH*, and *yjbIH* strains as compared to the wild-type strain. These data suggested that under the conditions examined, YjbIH influenced the activity of AcnA. It is possible that AcnA was not properly maturated into

410 a holo-protein in the *yjbH* and *yjbIH* strains. This possibility may have resulted from
411 decreased iron availability and incorporation into the AcnA [Fe-S] cluster. To gain
412 insight, we subjected the mutant strains to treatment with the cell-permeable, divalent
413 metal chelator 2,2-dipyrydyl (DIP), which has a high affinity for iron. An *fhuA* mutant,
414 which is defective in iron uptake was included as a control. As seen in Figure 5D, the
415 *yjbH*, *yjbIH*, and *fhuA* strains were more susceptible to treatment with DIP.
416
417 **The YjbH cysteine residues have no effect on pigmentation or Aur activity.**
418 Previous studies have investigated the contribution of the cysteine residues in YjbH to
419 its function, as cysteines are often redox-active and important for maintaining a reduced
420 environment. Göhring et al. (88) found that a *yjbH* mutant has a two-fold higher diamide
421 IC_{90S} compared to the wild-type strain that could not be complemented when the four
422 Cys residues in YjbH were mutated to glycines, yet they were not essential for
423 resistance to oxacillin. Conversely, Engman, et al. (53) reported that mutation of the Cys
424 residues to serines did not alter cellular levels of Spx after treatment with diamide. We
425 sought to investigate the role of the cysteines in *S. aureus* strain LAC. Upon
426 examination of the YjbH sequence, we hypothesized that there exist two thioredoxin
427 (Trx)-like motifs, $S^{44}xxC^{47}$ and $S^{118}xxC^{121}$ (Figure S5A). Trx active site motifs (CxxC)
428 often contain Ser substitutions in place of Cys residues (89, 90). To examine if these
429 Cys-containing, Trx-like motifs contributed to our *yjbH* mutant phenotypes, the Ser and
430 Cys residues were changed to alanines. The mutant motifs were introduced either
431 separately or together and used to complement the pigment and Aur phenotypes of the
432 *yjbH* mutant strain. As seen in Figure S5B & C, the mutation of either motif singly or in

433 combination was able to complement the *yjbH* mutant, indicating that they are
434 dispensable for YjbH-mediated regulation of pigment and Aur activity in *S. aureus* LAC.
435
436 **Contribution of Spx to the *yjbIH* mutant phenotypes.** The described function
437 of YjbH is to target Spx for degradation by the ClpXP protease (53, 91). Spx is an
438 essential protein in *S. aureus*, unless *trxA* is over-expressed. To test whether Spx
439 contributes to the *yjbIH* mutant phenotypes, we constructed mutants that also contain a
440 plasmid with *trxA* expressed from a non-native promoter (64). We found that an *spx*
441 mutant had similar pigment and Aur activity as the wild-type strain; however, deletion of
442 *spx* in a *yjbIH* mutant background rescued the pigment and Aur phenotypes of the *yjbIH*
443 mutant, indicating that these defects are Spx-dependent (Fig. 6A & B).
444 Complementation of the *yjbIH spx* mutant with *spx*$^{+}$ resulted in a pigment phenotype
445 similar to the *yjbIH* mutant and reduced the Aur activity of the *yjbIH spx* mutant back
446 towards that of the *yjbIH* mutant. Thus, these data suggested that increased Spx levels
447 as a result of the absence of YjbH leads to decreased pigment and Aur activity. Spx
448 levels are regulated by ClpXP machinery; therefore, we analyzed the effect of a *clpP*
449 deletion in our *yjbIH* mutant strain. We hypothesized that a *clpP* mutant would behave
450 similarly to a *yjbIH* mutant, since both strains would be expected to have increased
451 levels of Spx. Indeed, we observed that *clpP* and *yjbIH* mutants have similar pigment
452 and Aur phenotypes as shown in Figure 6A and B.
453 We exposed the *spx* mutant to disulfide stress, and as shown previously (64, 78),
454 we observed that the *spx* mutant was more sensitive to diamide than the wild-type strain
455 (Fig. 6C). Interestingly, the *spx yjbIH* mutant displayed increased resistance to diamide

as compared to the *spx*-only mutant. This result suggests that YjbIH may have additional targets other than Spx that contribute to disulfide stress. No difference was observed for the *yjbIH* mutant relative to wild-type. Together, these data demonstrated that Spx contributes to the altered pigment production and Aur expression seen in *yjbIH* mutant. However, the finding that the *yjbIH spx* double mutant phenocopies the *yjbIH* in diamide sensitivity, and not the *spx* single mutant, suggested that other factors are involved.

A role for σ^B in YjbIH-mediated regulation. The alternative sigma factor, σ^B (SigB) is the stress-response sigma factor in *S. aureus* and contributes to the regulation of both *crtOPQMN* and *aur*. σ^B is the primary activator of the staphyloxanthin biosynthesis operon, whereas it represses transcription of *aur* through SarA activation (28, 29, 36, 37). We wanted to determine if there was a relationship between the observed *yjbIH* mutant phenotypes and σ^B. We constructed a *yjbIH sigB* mutant and compared Aur activity and pigment among the strains. As expected, the absence of *sigB* in a wild-type background resulted in de-repression of Aur and reduced pigmentation (Figure 7). However, the enhanced proteolysis observed in the *sigB* mutant was eliminated when *yjbIH* was also absent. As for pigmentation, the *yjbIH sigB* strain appeared similar to the *sigB*-only mutant, with a near loss of staphyloxanthin production. Thus, while the loss of σ^B lead to decreased pigmentation regardless of YjbIH, enhanced proteolysis in the absence of σ^B was YjbIH-dependent.

The *yjbH* strain has increased resistance to superoxide and increased sensitivity to divalent metal deprivation (Fig. 4 & 5). We tested if these altered sensitivities were

dependent on *sigB* (Fig. 8A-B). In contrast to the *yjbH*-only mutant strain, we observed increased resistance to iron deprivation in the *yjbH sigB* strain to levels comparable to the *sigB* single mutant. The *sigB* mutant was extremely sensitive to methyl viologen; however, this appeared to be YjbH-dependent as the *yjbH* single and *yjbH sigB* mutants were equally more resistant than the *sigB* mutant. To further explore the link between σ^B and YjbIH, we tested if σ^B contributes to the decreased aconitase activity in the mutant strains (Fig. 8C). We observed decreased AcnA activity relative to the wild-type strain in all mutants except the *yjbI* mutant, with the *sigB* strain having the least activity. The decrease in AcnA activity was indistinguishable between the *yjbH* and *yjbH sigB* strains.

To further explore the connection between σ^B, YjbIH, and Spx, we introduced the *sigB* mutation into the *spx* mutant and *yjbIH* mutant backgrounds. We tested these mutant strains for pigmentation and Aur activity. The *sigB* mutation appeared to be dominant over both *spx* and *yjbIH* mutations, as both the *spx sigB* and *spx sigB yjbIH* strains have dramatically reduced pigmentation (Figure 9). Additionally, the lack of *sigB* appeared to be the major contributor to the de-repression of Aur activity in the *spx sigB* and *spx sigB yjbIH* strains. This contrasts with Aur activity observed in the *sigB yjbIH* mutant alone (Fig. 7), where the *yjbIH* mutation was dominant over *sigB*.

Deletion of *yjbIH* results in increased colonization in a murine sepsis model. During infection, *S. aureus* must combat a potent immune response that includes oxidative and nitrosative stress and other factors of the host immune system. Previous reports have found a role for proteases during infection, including Aur (12, 25). Furthermore, the absence of *S. aureus* proteases, such as Aur, leads to the stabilization

of virulence factors (12). Considering our observed phenotypes for the *yjbIH* mutant, we predicted that the YjbI and/or YjbH proteins would play a role during infection. To test this, we challenged the *yjbIH* strain using a murine sepsis model. We first administered a low-dose inoculum of wild-type and mutant strains separately. Surprisingly, we found that the *yjbIH* strain persisted in the kidneys after 6 days, whereas the wild-type strain was cleared by the host (Fig. 10A). We repeated the assay with a higher dose and found a similar trend (Fig. 10B). Higher titers of the *yjbIH* mutant strain were found in the kidneys and spleens, but not the livers. Mice infected with the mutant strain had increased morbidity visually and were scored for fitness, with the mutant-infected mice having a nearly two-fold decrease in fitness (data not shown). Additionally, the *yjbIH*-infected mice had about a 25% increase in weight loss as compared to the wild-type strain. In a separate experiment, we demonstrated the increased kidney bacterial burden found in the *yjbIH* mutant was restored when *yjbIH* was expressed on a plasmid (Fig. 10C).

We wanted to evaluate the individual contributions of *yjbI* and *yjbH* to the increased colonization ability observed for the *yjbIH* mutant. Therefore, we introduced the individual mutants into the mice. Both the *yjbI* and *yjbH* mutants trended towards higher bacteria numbers, although neither reached statistical significance (Fig. 10C). Together, these data demonstrated that the absence of YjbIH resulted in enhanced colonization of animals during a systemic infection.

DISCUSSION

524 YjbI remains unstudied in *S. aureus* and only a few reports exist on YjbH, mostly
525 due to identification in various screens for sensitivity to $NO^{\cdot}$ stress, desiccation, and
526 antibiotic resistance (83, 88, 92, 93). Based mostly on studies in *Bacillus*, YjbH is known
527 as an adaptor protein that targets Spx for degradation via the ClpXP protease (52, 53).
528 While YjbH has been linked to pigment changes (53), the mechanism was unknown and
529 no studies have linked YjbI or YjbH to Aur activity. Here, we demonstrate that YjbH
530 influences activation of both the *crtOPQMN* and *aur* promoters and this effect is most
531 likely exerted through either direct or indirect regulation by Spx and involves σ^B.
532 Interestingly, CrtOPQMN proteins were not identified as being altered during a
533 proteomic analysis of an *spx* mutant (78), yet the *yjbH* mutant phenotypes we observed
534 in this study are linked to Spx. As discussed below, this could be due to strain
535 differences or the result of the previous report using a σ^B-deficient strain that also
536 contained an unknown mutation in *rpoB*. Additionally, proteomic studies with a *clp*
537 mutant and Clp-trapping experiments did not identify CrtOPQMN or Aur as being altered
538 by the absence of *clp* or as potential Clp-binding targets (94, 95). Our study has
539 revealed novel roles for both YjbH and YjbI, and the data are consistent with a role for
540 Spx in controlling pigment and Aur. We also noted altered susceptibilities to $NO\cdot$, H_2O_2,
541 superoxide, and dipyridyl, but not diamide in a strain lacking YjbH. Some of the altered
542 susceptibilities and phenotypes observed are connected to σ^B despite no known
543 interaction between YjbH and σ^B. Finally, we demonstrate for the first time that a *yjbIH*
544 mutant has altered virulence in a murine model of infection.

545 Although the *S. aureus* and *B. subtilis* YjbH proteins are highly similar, there are
546 conflicting data about the role of the four cysteines in *S. aureus* YjbH function. Göhring,

et al. substituted Gly for each Cys residues and observed that they were required for resistance to diamide, but not resistance to oxacillin (88). However, Engman, et al. replaced the Cys residues with Ser and found that the Cys-free variants could complement Spx levels in a *B. subtilis yjbH* mutant with and without diamide treatment (53). Unlike the single motif in the *B. subtilis* YjbH, our analysis of the *S. aureus* YjbH suggests that there may be two thioredoxin-like motifs ($S^{44}xxC^{47}$ and $S^{118}xxC^{121}$) present. It is important to note that Trx motifs can have Ser substitutions at either terminus. We also speculate that there may be an active $C^{121}xC^{123}$ motif characteristic of the YphP disulfide isomerase found in *B. subtilis* (96). This CxC motif is found only in the *S. aureus* YjbH. In our studies, we exchanged the Ser and Cys residues of the SxxC motifs for Ala and found that these substitutions did not affect pigment or Aur activity under the conditions of our experiments. Thus, our studies are consistent with the work of Engman et al. (53), indicating no role for these cysteines in our observed phenotypes. However, it is likely that these Cys residues play a role in YjbH biology and that they only contribute to certain phenotypes as suggested by Göhring, et al. (88). Furthermore, the Cys residues may be essential for the predicted thiol-disulfide oxidoreductase activity of YjbH, which may not play a role in the observed Aur or pigment phenotypes. This may be similar to the chaperone-like functions found for thioredoxin that are independent of Cys residues. Future studies will be needed to reconcile the differences observed as to the importance of these cysteines in *S. aureus* YjbH function.

Spx has been well studied in *B. subtilis*, where is has been shown to be a transcriptional regulator that controls more than 140 transcriptional units (275 genes), including *trxA*, *trxB*, and those involved in cysteine biosynthesis and oxidative stress

(47, 56). Intracellular Spx levels are carefully regulated at both the transcriptional and post-translational levels (53, 97, 98). Under non-stressful conditions, YjbH binds to Spx, allowing its C-terminus to be exposed and resulting in proteolysis by ClpXP (Fig. 11). However, upon stress, YjbH self-aggregates leading to an increase in Spx levels, which goes on to regulate transcription (Fig. 11A) (99). As mentioned, only one study thus far has examined proteins affected by inactivation of Spx in *S. aureus*. In contrast to *B. subtilis*, only 13 proteins in *S. aureus* were identified as consistently altered by an *spx* deletion (78). Interestingly, Asp23, the hallmark indicator of σ^B activity was decreased in the *spx* mutant (78, 100). As mentioned above, CrtOPQMN and Aur were notably absent from the list of identified proteins. The lack of Aur could be the result of it being a secreted protein. However, two important observations should be noted. First, the proteomics study was performed in the 8325-4 strain, which is σ^B-deficient due to a *rsbU* mutation. Considering that we identified a link between σ^B and YjbH in our studies, this could contribute to the lack of CrtOPQMN or Aur being identified during proteomic analysis. Second, it was recently found that *spx* is essential without controlled expression of TrxA or TrxB, and that the previous 8325-4 mutant had a secondary-site mutation in *rpoB* (64, 78). How this would influence analysis of the strain is unknown, but it may explain the differences between the previous studies and our results. As far as we are aware, our studies are the first to examine isogenic *yjbH* and *spx* mutants. How Spx alters pigment and Aur expression is unknown. The identification of Spx target promoters is difficult since Spx does not bind the promoter sequence itself, but in some way, directs RNAP to promoters via interactions with the RNAP α-CTD (55, 101). For *B. subtilis* Spx, targeting to the *trxB* promoter requires an AGCA and AGCG (101, 102) in

close proximity to the -35 region. Neither of these sequences can be found close to the identified -35 of the *aur* promoter (our analysis of published promoter (103)). Thus, additional studies will be needed to directly test this hypothesis and whether the effects of YjbH/Spx are direct on *crtOPQMN* and *aur* or acting through additional regulatory networks.

We identified a link between YjbH, Spx, and σ^B (Fig. 11B). Identifying an overlap or coordination between Spx and σ^B may not be surprising since both proteins alter gene expression in response to stress. σ^B controls expression of both *aur* and *crtOPQMN*, acting as a key repressor and activator, respectively. The simplest explanation for decreased pigmentation for the *yjbIH* mutant is that σ^B activity is decreased. However, σ^B represses *aur* expression, and if YjbH acted solely through σ^B activity, then the *yjbIH* mutant would be expected to have increased Aur expression, which is opposite of the results presented here. Alternatively, it is possible that the lack of YjbH leads to increased Spx levels, which directly affect σ^B activity. However, such a linear relationship cannot be explained by the data presented herein. It is interesting to note the dominance of YjbH and σ^B in the observed phenotypes. In Aur activity, the *yjbIH* mutant phenotype supersedes the *sigB* mutation. Yet, the opposite is true for pigmentation where the *sigB* mutation is dominant over the *yjbH* deletion. Thus, the relationship between YjbH, Spx, and σ^B must be more complex. This is likely true since *aur* is under complex regulation by multiple layers of regulatory networks. One scenario that does account for the pattern of Aur activity and pigment in our combination mutant strains is if σ^B and Spx independently act on the *aur* and *crtOPQMN* promoters. In this case, σ^B is a strong repressor of *aur* and activator of *crtOPQMN*. In the wild-type strain,

σ^B carefully controls the expression of both transcripts. However, when YjbH is absent, there is an increase in Spx levels that represses both *aur* and *crtOPQMN*. This would account for the dramatic drop in Aur activity in the *yjbIH* mutant as the two repressors (σ^B and Spx) are abundant. This could also account for the intermediate pigmentation phenotype of the *yjbIH* mutant since an increased abundance of the repressor, Spx, would be competing with σ^B-dependent activation. In this model, σ^B would have a stronger influence over the *aur* and *crtOPQMN* promoters than Spx. This model would also account for the finding that the *sigB* mutation is dominant over both *spx* and *yjbIH* mutations in pigment, yet the *yjbIH* mutant is dominant over the *sigB* mutation in Aur activity. Considering the complexity of overlapping regulatory networks in *S. aureus*, it is quite possible that additional regulatory systems are involved. For example, an alternative model could exist where YjbH manifests some phenotypes through an unknown activator. For example, in the absence of the major repressor, σ^B, *aur* expression increases because the promoter is accessible to an activator. This activator's activity would by modulated by YjbH, explaining the loss of Aur activity in the *yjbH sigB* mutant. Another interesting possibility exists regarding how Spx acts to alter gene transcription. As mentioned above, Spx interacts with RNAP directly and not DNA. It is thought that this affects the ability of transcriptional regulators to interact with RNAP. Whether this could also affect incorporation of the sigma subunit remains unclear. Our data generates multiple testable models that will require further investigation to identify the exact mechanism by which YjbH-mediated phenotypes manifest.

638 The studies herein are the first to examine the contribution of YjbIH to virulence.
639 Based on our *in vitro* data, multiple possible outcomes were predicted. First, it was
640 possible that the mutant would have reduced virulence due to decreased resistance to
641 RNS or H_2O_2. However, the mutant was more resistant to superoxide (Fig. 4C), making
642 it difficult to anticipate how this would affect infection outcomes. Second, the mutant has
643 decreased production of the Aur protease which would affect colonization. It should be
644 noted that Aur is known to initiate a protease cascade, including SspA (V8) and SspB
645 (22); therefore, the absence of Aur would be expected to decrease the activity of those
646 proteases. Importantly, *S. aureus* proteases play many roles for the bacterium, including
647 targeting host defenses and modulating extracellular virulence factors (11-21). Indeed,
648 absence of the Aur, SspA, SspB, ScpA and SplA-F proteases increases the abundance
649 of secreted and surface-associated virulence factors (12). Interestingly, this same study
650 noted that the strain lacking all proteases is protected from leukocytes, granulocytes,
651 and monocytes and led to decreased survival of mice during a systemic murine infection
652 model similar to that used in our study. In addition, inactivation of Aur has been shown
653 to increase the abundance of 225 Sae-regulated proteins (25). Thus, the absence of
654 Aur would be expected to decrease the degradation of host proteins, but at the same
655 time, increase the abundance of virulence factors. Based on these published studies, it
656 is possible that since the *yjbIH* mutant has decreased Aur expression, this leads to
657 stabilization of virulence factors *in vivo*, and consequently, enhanced virulence. The *in*
658 *vivo* environment is complex and dynamic, with changing environments and host factors
659 in different niches and, therefore, the true nature of this interaction is likely not as simple
660 as we propose. Testing this hypothesis is one component of ongoing studies.

ACKNOWLEDGEMENTS

We thank Drs. Kelly Rice (University of Florida) and Ronan Carroll (Ohio University) for their valuable discussions, suggestions, and expertise. In addition, we would like to thank Dr. William Kelley at the University Hospital and Medical School of Geneva for providing strains CB1400 and MV58, as well as Dr. Alex Horswill at University of Colorado Anschutz Medical Campus for AH1358. This study was funded by the University of Kansas Medical Center and, in part, by funding from the National Institute of Allergy and Infectious Diseases (NIAID) award R01AI121073 to JLB, and a pilot project grant through award P20GM112117. The Boyd lab is funded by NIAID award 1R01AI139100-01, NSF award MCB-1750624, and USDA MRF project NE-1028.

REFERENCES

1. Fowler VG, Jr., Miro JM, Hoen B, Cabell CH, Abrutyn E, Rubinstein E, Corey GR, Spelman D, Bradley SF, Barsic B, Pappas PA, Anstrom KJ, Wray D, Fortes CQ, Anguera I, Athan E, Jones P, van der Meer JT, Elliott TS, Levine DP, Bayer AS, Investigators ICE. 2005. *Staphylococcus aureus* endocarditis: a consequence of medical progress. JAMA 293:3012-21.
2. Montanaro L, Speziale P, Campoccia D, Ravaioli S, Cangini I, Pietrocola G, Giannini S, Arciola CR. 2011. Scenery of *Staphylococcus* implant infections in orthopedics. Future Microbiol 6:1329-49.

3. Moran GJ, Krishnadasan A, Gorwitz RJ, Fosheim GE, McDougal LK, Carey RB, Talan DA, Group EMINS. 2006. Methicillin-resistant *S. aureus* infections among patients in the emergency department. N Engl J Med 355:666-74.
4. Wisplinghoff H, Bischoff T, Tallent SM, Seifert H, Wenzel RP, Edmond MB. 2004. Nosocomial bloodstream infections in US hospitals: analysis of 24,179 cases from a prospective nationwide surveillance study. Clin Infect Dis 39:309-17.
5. Lowy FD. 1998. *Staphylococcus aureus* infections. N Engl J Med 339:520-32.
6. Bronner S, Monteil H, Prevost G. 2004. Regulation of virulence determinants in *Staphylococcus aureus*: complexity and applications. FEMS Microbiol Rev 28:183-200.
7. Diep BA, Otto M. 2008. The role of virulence determinants in community-associated MRSA pathogenesis. Trends Microbiol 16:361-9.
8. Montgomery CP, Boyle-Vavra S, Adem PV, Lee JC, Husain AN, Clasen J, Daum RS. 2008. Comparison of virulence in community-associated methicillin-resistant *Staphylococcus aureus* pulsotypes USA300 and USA400 in a rat model of pneumonia. J Infect Dis 198:561-70.
9. Kobayashi SD, DeLeo FR. 2009. An update on community-associated MRSA virulence. Curr Opin Pharmacol 9:545-51.
10. Li M, Diep BA, Villaruz AE, Braughton KR, Jiang X, DeLeo FR, Chambers HF, Lu Y, Otto M. 2009. Evolution of virulence in epidemic community-associated methicillin-resistant *Staphylococcus aureus*. Proc Natl Acad Sci U S A 106:5883-8.

11. Karlsson A, Saravia-Otten P, Tegmark K, Morfeldt E, Arvidson S. 2001. Decreased amounts of cell wall-associated protein A and fibronectin-binding proteins in *Staphylococcus aureus sarA* mutants due to up-regulation of extracellular proteases. Infect Immun 69:4742-8.
12. Kolar SL, Ibarra JA, Rivera FE, Mootz JM, Davenport JE, Stevens SM, Horswill AR, Shaw LN. 2013. Extracellular proteases are key mediators of *Staphylococcus aureus* virulence via the global modulation of virulence-determinant stability. Microbiologyopen 2:18-34.
13. McAleese FM, Walsh EJ, Sieprawska M, Potempa J, Foster TJ. 2001. Loss of clumping factor B fibrinogen binding activity by *Staphylococcus aureus* involves cessation of transcription, shedding and cleavage by metalloprotease. J Biol Chem 276:29969-78.
14. Jusko M, Potempa J, Kantyka T, Bielecka E, Miller HK, Kalinska M, Dubin G, Garred P, Shaw LN, Blom AM. 2014. Staphylococcal proteases aid in evasion of the human complement system. J Innate Immun 6:31-46.
15. Laarman AJ, Mijnheer G, Mootz JM, van Rooijen WJ, Ruyken M, Malone CL, Heezius EC, Ward R, Milligan G, van Strijp JA, de Haas CJ, Horswill AR, van Kessel KP, Rooijakkers SH. 2012. *Staphylococcus aureus* staphopain A inhibits CXCR2-dependent neutrophil activation and chemotaxis. EMBO J 31:3607-19.
16. Massimi I, Park E, Rice K, Muller-Esterl W, Sauder D, McGavin MJ. 2002. Identification of a novel maturation mechanism and restricted substrate specificity for the SspB cysteine protease of *Staphylococcus aureus*. J Biol Chem 277:41770-7.

17. Ohbayashi T, Irie A, Murakami Y, Nowak M, Potempa J, Nishimura Y, Shinohara M, Imamura T. 2011. Degradation of fibrinogen and collagen by staphopains, cysteine proteases released from *Staphylococcus aureus*. Microbiology 157:786-92.

18. Potempa J, Dubin A, Korzus G, Travis J. 1988. Degradation of elastin by a cysteine proteinase from *Staphylococcus aureus*. J Biol Chem 263:2664-7.

19. Potempa J, Watorek W, Travis J. 1986. The inactivation of human plasma alpha 1-proteinase inhibitor by proteinases from *Staphylococcus aureus*. J Biol Chem 261:14330-4.

20. Prokesova L, Potuznikova B, Potempa J, Zikan J, Radl J, Hachova L, Baran K, Porwit-Bobr Z, John C. 1992. Cleavage of human immunoglobulins by serine proteinase from *Staphylococcus aureus*. Immunol Lett 31:259-65.

21. Sieprawska-Lupa M, Mydel P, Krawczyk K, Wojcik K, Puklo M, Lupa B, Suder P, Silberring J, Reed M, Pohl J, Shafer W, McAleese F, Foster T, Travis J, Potempa J. 2004. Degradation of human antimicrobial peptide LL-37 by *Staphylococcus aureus*-derived proteinases. Antimicrob Agents Chemother 48:4673-9.

22. Nickerson NN, Prasad L, Jacob L, Delbaere LT, McGavin MJ. 2007. Activation of the SspA serine protease zymogen of *Staphylococcus aureus* proceeds through unique variations of a trypsinogen-like mechanism and is dependent on both autocatalytic and metalloprotease-specific processing. J Biol Chem 282:34129-38.

23. Rice K, Peralta R, Bast D, de Azavedo J, McGavin MJ. 2001. Description of staphylococcus serine protease (*ssp*) operon in *Staphylococcus aureus* and nonpolar inactivation of *sspA*-encoded serine protease. Infect Immun 69:159-69.
24. Laarman AJ, Ruyken M, Malone CL, van Strijp JA, Horswill AR, Rooijakkers SH. 2011. *Staphylococcus aureus* metalloprotease aureolysin cleaves complement C3 to mediate immune evasion. J Immunol 186:6445-53.
25. Cassat JE, Hammer ND, Campbell JP, Benson MA, Perrien DS, Mrak LN, Smeltzer MS, Torres VJ, Skaar EP. 2013. A secreted bacterial protease tailors the *Staphylococcus aureus* virulence repertoire to modulate bone remodeling during osteomyelitis. Cell Host Microbe 13:759-72.
26. Oscarsson J, Tegmark-Wisell K, Arvidson S. 2006. Coordinated and differential control of aureolysin (*aur*) and serine protease (*sspA*) transcription in *Staphylococcus aureus* by *sarA*, *rot* and *agr* (RNAIII). Int J Med Microbiol 296:365-80.
27. Karlsson A, Arvidson S. 2002. Variation in extracellular protease production among clinical isolates of *Staphylococcus aureus* due to different levels of expression of the protease repressor *sarA*. Infect Immun 70:4239-46.
28. Deora R, Tseng T, Misra TK. 1997. Alternative transcription factor sigmaSB of *Staphylococcus aureus*: characterization and role in transcription of the global regulatory locus *sar*. J Bacteriol 179:6355-9.
29. Bischoff M, Entenza JM, Giachino P. 2001. Influence of a functional *sigB* operon on the global regulators *sar* and *agr* in *Staphylococcus aureus*. J Bacteriol 183:5171-9.

30. Rogasch K, Ruhmling V, Pane-Farre J, Hoper D, Weinberg C, Fuchs S, Schmudde M, Broker BM, Wolz C, Hecker M, Engelmann S. 2006. Influence of the two-component system SaeRS on global gene expression in two different *Staphylococcus aureus* strains. J Bacteriol 188:7742-58.

31. El-Agamey A, Lowe GM, McGarvey DJ, Mortensen A, Phillip DM, Truscott TG, Young AJ. 2004. Carotenoid radical chemistry and antioxidant/pro-oxidant properties. Arch Biochem Biophys 430:37-48.

32. Grinsted J, Lacey RW. 1973. Ecological and genetic implications of pigmentation in *Staphylococcus aureus*. J Gen Microbiol 75:259-67.

33. Liu GY, Essex A, Buchanan JT, Datta V, Hoffman HM, Bastian JF, Fierer J, Nizet V. 2005. *Staphylococcus aureus* golden pigment impairs neutrophil killing and promotes virulence through its antioxidant activity. J Exp Med 202:209-15.

34. Clauditz A, Resch A, Wieland KP, Peschel A, Gotz F. 2006. Staphyloxanthin plays a role in the fitness of *Staphylococcus aureus* and its ability to cope with oxidative stress. Infect Immun 74:4950-3.

35. Hampton MB, Kettle AJ, Winterbourn CC. 1998. Inside the neutrophil phagosome: oxidants, myeloperoxidase, and bacterial killing. Blood 92:3007-17.

36. Pelz A, Wieland KP, Putzbach K, Hentschel P, Albert K, Gotz F. 2005. Structure and biosynthesis of staphyloxanthin from *Staphylococcus aureus*. J Biol Chem 280:32493-8.

37. Bischoff M, Dunman P, Kormanec J, Macapagal D, Murphy E, Mounts W, Berger-Bachi B, Projan S. 2004. Microarray-based analysis of the *Staphylococcus aureus* sigmaB regulon. J Bacteriol 186:4085-99.

794 38. Liu Y, Wu N, Dong J, Gao Y, Zhang X, Shao N, Yang G. 2010. SsrA (tmRNA)
795 acts as an antisense RNA to regulate *Staphylococcus aureus* pigment synthesis
796 by base pairing with *crtMN* mRNA. FEBS Lett 584:4325-9.
797 39. Hausladen A, Gow A, Stamler JS. 2001. Flavohemoglobin denitrosylase
798 catalyzes the reaction of a nitroxyl equivalent with molecular oxygen. Proc Natl
799 Acad Sci U S A 98:10108-12.
800 40. Richardson AR, Dunman PM, Fang FC. 2006. The nitrosative stress response of
801 *Staphylococcus aureus* is required for resistance to innate immunity. Mol
802 Microbiol 61:927-39.
803 41. Clements MO, Watson SP, Foster SJ. 1999. Characterization of the major
804 superoxide dismutase of *Staphylococcus aureus* and its role in starvation
805 survival, stress resistance, and pathogenicity. J Bacteriol 181:3898-903.
806 42. Karavolos MH, Horsburgh MJ, Ingham E, Foster SJ. 2003. Role and regulation of
807 the superoxide dismutases of *Staphylococcus aureus*. Microbiology 149:2749-58.
808 43. Martin SE, Chaven S. 1987. Synthesis of catalase in *Staphylococcus aureus* MF-
809 31. Appl Environ Microbiol 53:1207-9.
810 44. Cosgrove K, Coutts G, Jonsson IM, Tarkowski A, Kokai-Kun JF, Mond JJ, Foster
811 SJ. 2007. Catalase (KatA) and alkyl hydroperoxide reductase (AhpC) have
812 compensatory roles in peroxide stress resistance and are required for survival,
813 persistence, and nasal colonization in *Staphylococcus aureus*. J Bacteriol
814 189:1025-35.
815 45. Holmgren A. 1989. Thioredoxin and glutaredoxin systems. J Biol Chem
816 264:13963-6.

46. Chaudhuri RR, Allen AG, Owen PJ, Shalom G, Stone K, Harrison M, Burgis TA, Lockyer M, Garcia-Lara J, Foster SJ, Pleasance SJ, Peters SE, Maskell DJ, Charles IG. 2009. Comprehensive identification of essential *Staphylococcus aureus* genes using Transposon-Mediated Differential Hybridisation (TMDH). BMC Genomics 10:291.

47. Uziel O, Borovok I, Schreiber R, Cohen G, Aharonowitz Y. 2004. Transcriptional regulation of the *Staphylococcus aureus* thioredoxin and thioredoxin reductase genes in response to oxygen and disulfide stress. J Bacteriol 186:326-34.

48. Singh VK, Moskovitz J. 2003. Multiple methionine sulfoxide reductase genes in *Staphylococcus aureus*: expression of activity and roles in tolerance of oxidative stress. Microbiology 149:2739-47.

49. Singh VK, Moskovitz J, Wilkinson BJ, Jayaswal RK. 2001. Molecular characterization of a chromosomal locus in *Staphylococcus aureus* that contributes to oxidative defence and is highly induced by the cell-wall-active antibiotic oxacillin. Microbiology 147:3037-45.

50. Fey PD, Endres JL, Yajjala VK, Widhelm TJ, Boissy RJ, Bose JL, Bayles KW. 2013. A genetic resource for rapid and comprehensive phenotype screening of nonessential *Staphylococcus aureus* genes. MBio 4:e00537-12.

51. Kelley LA, Sternberg MJ. 2009. Protein structure prediction on the web: a case study using the Phyre server. Nat Protoc 4:363-71.

52. Larsson JT, Rogstam A, von Wachenfeldt C. 2007. YjbH is a novel negative effector of the disulphide stress regulator, Spx, in *Bacillus subtilis*. Mol Microbiol 66:669-84.

840 53. Engman J, Rogstam A, Frees D, Ingmer H, von Wachenfeldt C. 2012. The YjbH
841 adaptor protein enhances proteolysis of the transcriptional regulator Spx in
842 *Staphylococcus aureus*. J Bacteriol 194:1186-94.
843 54. Nakano S, Kuster-Schock E, Grossman AD, Zuber P. 2003. Spx-dependent
844 global transcriptional control is induced by thiol-specific oxidative stress in
845 *Bacillus subtilis*. Proc Natl Acad Sci U S A 100:13603-8.
846 55. Zuber P. 2004. Spx-RNA polymerase interaction and global transcriptional
847 control during oxidative stress. J Bacteriol 186:1911-8.
848 56. Rochat T, Nicolas P, Delumeau O, Rabatinova A, Korelusova J, Leduc A,
849 Bessieres P, Dervyn E, Krasny L, Noirot P. 2012. Genome-wide identification of
850 genes directly regulated by the pleiotropic transcription factor Spx in *Bacillus*
851 *subtilis*. Nucleic Acids Res 40:9571-83.
852 57. Hanahan D. 1983. Studies on transformation of *Escherichia coli* with plasmids. J
853 Mol Biol 166:557-80.
854 58. Dunn AK, Martin MO, Stabb EV. 2005. Characterization of pES213, a small
855 mobilizable plasmid from *Vibrio fischeri*. Plasmid 54:114-34.
856 59. Bose JL, Fey PD, Bayles KW. 2013. Genetic tools to enhance the study of gene
857 function and regulation in *Staphylococcus aureus*. Appl Environ Microbiol
858 79:2218-24.
859 60. Kreiswirth BN, Lofdahl S, Betley MJ, O'Reilly M, Schlievert PM, Bergdoll MS,
860 Novick RP. 1983. The toxic shock syndrome exotoxin structural gene is not
861 detectably transmitted by a prophage. Nature 305:709-12.

862 61. Krausz KL, Bose JL. 2016. Bacteriophage Transduction in *Staphylococcus*
863 *aureus*: Broth-Based Method. Methods Mol Biol 1373:63-8.
864 62. Bose JL. 2014. Genetic manipulation of staphylococci. Methods Mol Biol
865 1106:101-11.
866 63. Krausz KL, Bose JL. 2016. Rapid Isolation of DNA from *Staphylococcus*.
867 Methods Mol Biol 1373:59-62.
868 64. Villanueva M, Jousselin A, Baek KT, Prados J, Andrey DO, Renzoni A, Ingmer H,
869 Frees D, Kelley WL. 2016. Rifampin resistance *rpoB* alleles or multicopy
870 thioredoxin/thioredoxin reductase suppresses the lethality of disruption of the
871 global stress regulator *spx* in *Staphylococcus aureus*. J Bacteriol 198:2719-31.
872 65. Krute CN, Krausz KL, Markiewicz MA, Joyner JA, Pokhrel S, Hall PR, Bose JL.
873 2016. Generation of a stable plasmid for *in vitro* and *in vivo* studies of
874 *Staphylococcus*. Appl Environ Microbiol doi:10.1128/AEM.02370-16.
875 66. Morikawa K, Maruyama A, Inose Y, Higashide M, Hayashi H, Ohta T. 2001.
876 Overexpression of sigma factor, sigma(B), urges *Staphylococcus aureus* to
877 thicken the cell wall and to resist beta-lactams. Biochem Biophys Res Commun
878 288:385-9.
879 67. Sapp AM, Mogen AB, Almand EA, Rivera FE, Shaw LN, Richardson AR, Rice
880 KC. 2014. Contribution of the *nos-pdt* operon to virulence phenotypes in
881 methicillin-sensitive *Staphylococcus aureus*. PLoS One 9:e108868.
882 68. Krute CN, Rice KC, Bose JL. 2017. VfrB is a key activator of the *Staphylococcus*
883 *aureus* SaeRS two-component system. J Bacteriol 199:e00828-16.

884 69. Lehman MK, Bose JL, Sharma-Kuinkel BK, Moormeier DE, Endres JL, Sadykov
885 MR, Biswas I, Bayles KW. 2015. Identification of the amino acids essential for
886 LytSR-mediated signal transduction in *Staphylococcus aureus* and their roles in
887 biofilm-specific gene expression. Mol Microbiol 95:723-37.
888 70. Bose JL, Daly SM, Hall PR, Bayles KW. 2014. Identification of the
889 *Staphylococcus aureus vfrAB* operon, a novel virulence factor regulatory locus.
890 Infect Immun 82:1813-22.
891 71. Livak KJ, Schmittgen TD. 2001. Analysis of relative gene expression data using
892 real-time quantitative PCR and the 2(-Delta Delta C(T)) Method. Methods
893 25:402-8.
894 72. Moormeier DE, Endres JL, Mann EE, Sadykov MR, Horswill AR, Rice KC, Fey
895 PD, Bayles KW. 2013. Use of microfluidic technology to analyze gene expression
896 during *Staphylococcus aureus* biofilm formation reveals distinct physiological
897 niches. Appl Environ Microbiol 79:3413-24.
898 73. Lewis AM, Rice KC. 2016. Quantitative real-time PCR (qPCR) workflow for
899 analyzing *Staphylococcus aureus* gene expression. Methods Mol Biol 1373:143-
900 54.
901 74. Grosser MR, Weiss A, Shaw LN, Richardson AR. 2016. Regulatory requirements
902 for *Staphylococcus aureus* nitric oxide resistance. J Bacteriol 198:2043-55.
903 75. Mashruwala AA, Pang YY, Rosario-Cruz Z, Chahal HK, Benson MA, Mike LA,
904 Skaar EP, Torres VJ, Nauseef WM, Boyd JM. 2015. Nfu facilitates the maturation
905 of iron-sulfur proteins and participates in virulence in *Staphylococcus aureus*. Mol
906 Microbiol 95:383-409.

907 76. Mashruwala AA, Bhatt S, Poudel S, Boyd ES, Boyd JM. 2016. The DUF59
908 containing protein SufT is involved in the maturation of iron-sulfur (FeS) proteins
909 during conditions of high FeS cofactor demand in *Staphylococcus aureus*. PLoS
910 Genet 12:e1006233.
911 77. Rosario-Cruz Z, Chahal HK, Mike LA, Skaar EP, Boyd JM. 2015. Bacillithiol has
912 a role in Fe-S cluster biogenesis in *Staphylococcus aureus*. Mol Microbiol
913 98:218-42.
914 78. Pamp SJ, Frees D, Engelmann S, Hecker M, Ingmer H. 2006. Spx is a global
915 effector impacting stress tolerance and biofilm formation in *Staphylococcus*
916 *aureus*. J Bacteriol 188:4861-70.
917 79. Council NR. 2011. Guide for the care and use of laboratory animals, 8th ed.
918 National Academies Press, Washington, DC.
919 80. Bustamante JP, Radusky L, Boechi L, Estrin DA, Ten Have A, Marti MA. 2016.
920 Evolutionary and functional relationships in the truncated hemoglobin family.
921 PLoS Comput Biol 12:e1004701.
922 81. Ouellet H, Ranguelova K, Labarre M, Wittenberg JB, Wittenberg BA, Magliozzo
923 RS, Guertin M. 2007. Reaction of *Mycobacterium tuberculosis* truncated
924 hemoglobin O with hydrogen peroxide: evidence for peroxidatic activity and
925 formation of protein-based radicals. J Biol Chem 282:7491-503.
926 82. Wittenberg JB, Bolognesi M, Wittenberg BA, Guertin M. 2002. Truncated
927 hemoglobins: a new family of hemoglobins widely distributed in bacteria,
928 unicellular eukaryotes, and plants. J Biol Chem 277:871-4.

83. Grosser MR, Paluscio E, Thurlow LR, Dillon MM, Cooper VS, Kawula TH, Richardson AR. 2018. Genetic requirements for *Staphylococcus aureus* nitric oxide resistance and virulence. PLoS Pathog 14:e1006907.
84. Beinert H, Kennedy MC, Stout CD. 1996. Aconitase as iron-sulfur protein, enzyme, and iron-regulatory protein. Chem Rev 96:2335-2374.
85. Imlay JA. 2006. Iron-sulphur clusters and the problem with oxygen. Mol Microbiol 59:1073-82.
86. Roberts CA, Al-Tameemi HM, Mashruwala AA, Rosario-Cruz Z, Chauhan U, Sause WE, Torres VJ, Belden WJ, Boyd JM. 2017. The suf iron-sulfur cluster biosynthetic system is essential in *Staphylococcus aureus*, and decreased suf function results in global metabolic defects and reduced survival in human neutrophils. Infect Immun 85:e00100-17.
87. Mashruwala AA, Boyd JM. 2017. The *Staphylococcus aureus* SrrAB regulatory system modulates hydrogen peroxide resistance factors, which imparts protection to aconitase during aerobic growth. PLoS One 12:e0170283.
88. Gohring N, Fedtke I, Xia G, Jorge AM, Pinho MG, Bertsche U, Peschel A. 2011. New role of the disulfide stress effector YjbH in beta-lactam susceptibility of *Staphylococcus aureus*. Antimicrob Agents Chemother 55:5452-8.
89. Atkinson HJ, Babbitt PC. 2009. An atlas of the thioredoxin fold class reveals the complexity of function-enabling adaptations. PLoS Comput Biol 5:e1000541.
90. Holmgren A, Johansson C, Berndt C, Lonn ME, Hudemann C, Lillig CH. 2005. Thiol redox control via thioredoxin and glutaredoxin systems. Biochem Soc Trans 33:1375-7.

91. Garg SK, Kommineni S, Henslee L, Zhang Y, Zuber P. 2009. The YjbH protein of *Bacillus subtilis* enhances ClpXP-catalyzed proteolysis of Spx. J Bacteriol 191:1268-77.
92. Chaibenjawong P, Foster SJ. 2011. Desiccation tolerance in *Staphylococcus aureus*. Arch Microbiol 193:125-35.
93. Ba X, Kalmar L, Hadjirin NF, Kerschner H, Apfalter P, Morgan FJ, Paterson GK, Girvan SL, Zhou R, Harrison EM, Holmes MA. 2019. Truncation of GdpP mediates beta-lactam resistance in clinical isolates of *Staphylococcus aureus*. J Antimicrob Chemother doi:10.1093/jac/dkz013:1-10.
94. Farrand AJ, Friedman DB, Reniere ML, Ingmer H, Frees D, Skaar EP. 2015. Proteomic analyses of iron-responsive, Clp-dependent changes in *Staphylococcus aureus*. Pathog Dis 73:ftv004.
95. Feng J, Michalik S, Varming AN, Andersen JH, Albrecht D, Jelsbak L, Krieger S, Ohlsen K, Hecker M, Gerth U, Ingmer H, Frees D. 2013. Trapping and proteomic identification of cellular substrates of the ClpP protease in *Staphylococcus aureus*. J Proteome Res 12:547-58.
96. Derewenda U, Boczek T, Gorres KL, Yu M, Hung LW, Cooper D, Joachimiak A, Raines RT, Derewenda ZS. 2009. Structure and function of *Bacillus subtilis* YphP, a prokaryotic disulfide isomerase with a CXC catalytic motif. Biochemistry 48:8664-71.
97. Leelakriangsak M, Zuber P. 2007. Transcription from the P3 promoter of the *Bacillus subtilis spx* gene is induced in response to disulfide stress. J Bacteriol 189:1727-35.

98. Leelakriangsak M, Kobayashi K, Zuber P. 2007. Dual negative control of spx transcription initiation from the P3 promoter by repressors PerR and YodB in *Bacillus subtilis*. J Bacteriol 189:1736-44.
99. Engman J, von Wachenfeldt C. 2015. Regulated protein aggregation: a mechanism to control the activity of the ClpXP adaptor protein YjbH. Mol Microbiol 95:51-63.
100. Giachino P, Engelmann S, Bischoff M. 2001. Sigma(B) activity depends on RsbU in *Staphylococcus aureus*. J Bacteriol 183:1843-52.
101. Nakano MM, Lin A, Zuber CS, Newberry KJ, Brennan RG, Zuber P. 2010. Promoter recognition by a complex of Spx and the C-terminal domain of the RNA polymerase alpha subunit. PLoS One 5:e8664.
102. Lin AA, Walthers D, Zuber P. 2013. Residue substitutions near the redox center of *Bacillus subtilis* Spx affect RNA polymerase interaction, redox control, and Spx-DNA contact at a conserved *cis*-acting element. J Bacteriol 195:3967-78.
103. Shaw L, Golonka E, Potempa J, Foster SJ. 2004. The role and regulation of the extracellular proteases of *Staphylococcus aureus*. Microbiology 150:217-28.
104. Boles BR, Thoendel M, Roth AJ, Horswill AR. 2010. Identification of genes involved in polysaccharide-independent *Staphylococcus aureus* biofilm formation. PLoS One 5:e10146.
105. Krute CN, Ridder MJ, Seawell NA, Bose JL. 2018. Inactivation of the exogenous fatty acid utilization pathway leads to increased resistance to unsaturated fatty acids in *Staphylococcus aureus*. Microbiology doi:10.1099/mic.0.000757.

106. Pang YY, Schwartz J, Thoendel M, Ackermann LW, Horswill AR, Nauseef WM. 2010. *agr*-Dependent interactions of *Staphylococcus aureus* USA300 with human polymorphonuclear neutrophils. J Innate Immun 2:546-59.

FIG 1. Staphyloxanthin production and Aur activity are reduced in the *yjbIH* and *yjbH* mutants. **(A)** Carotenoid pigment assay with representative photos of colony colors. Values are the averages of two independent experiments. Error bars represent SEM (*n* = 6). *, $p < 0.05$ and **, $p < 0.01$ according to a one-way ANOVA with Holm-Sidak's multiple comparison test. **(B)** Protease assay using 1.0% skim milk agar plates. Per panel, images are representative of > 3 independent experiments and are of cultures grown on the same plate and adjusted for contrast similarly.

FIG 2. β-Galactosidase activities of strains containing **(A, C)** *crtOPQMN* or **(B, D)** *aur* promoter-*lacZ* fusions. For (A) and (B), samples were taken over the course of growth until early stationary phase. For (C) and (D), cells were harvested after 8h of growth. Data are representative of $\geq$ 3 independent experiments. Error bars represent SEM (*n* = 3). **, $p < 0.01$ and * $p < 0.05$ as determined by Student's *t* test. For panel "A" the *sigB* mutant was statistically different than WT at all time points.

FIG 3. Sensitivity of mutants to $NO^{\cdot}$ stress. **(A)** Strains were grown in LBGT medium with (empty symbols) or without (closed symbols) 10 mM DETA-NO. Data is the average (*n* = 3) with SEM. **(B)** The area under the curve was calculated for each strain.

**, $p < 0.01$ and *, $p < 0.05$ according to a one-way ANOVA and Holm-Sidak's multiple comparisons test.

FIG 4. Altered sensitivities of strains to ROS. Serial dilutions of WT, *yjbI*, *yjbH*, and *yjbIH* mutant strains **(A)** untreated or exposed to **(B)** 1 M hydrogen peroxide or **(C)** 25 mM of superoxide-producing methyl viologen. "+con" indicates either a mutation in *katA* (panels A and B) or *sodM* (panel C) as controls.

FIG 5. Aconitase activity and sensitivity to Fe chelation. Aconitase activity in *yjbI, yjbH,* and *yjbIH* mutant strains as compared to the wild-type strain grown at **(A)** high and **(B)** low aeration. **(C)** Aconitase activity of *acnA* combination mutant strains with *acnA* expressed from a non-native promoter under high aeration. Data is the average (n = 3) with SD. *, $p < 0.05$ as compared to WT using a one-way ANOVA with Tukey's multiple comparison test. **(D)** Sensitivity of the mutant strains exposed to 1 mM of the metal chelator 2,2,-dipyridyl.

FIG 6. Relationship of *yjbIH* phenotypes to Spx and ClpP. **(A)** Colony pigment of strains grown overnight on TSA plates. **(B)** Aur activity assay using 1% skim milk agar plate. **(C)** Serial dilutions of indicated strains spotted onto TSA containing 0.2 mM diamide. Per panel, images are of cultures grown on the same plate and adjusted for contrast similarly. *spx*$^+$ indicates complementation of *spx* in the *yjbIH spx* double mutant.

FIG 7. Relationship of YjbIH and σ^B. Aur activity assay using 1% skim milk agar plate (left) and colony pigment of strains grown overnight on TSA plates (right). JLB174 is the *sigB* strain used. All images are of cultures grown on the same plates and adjusted for contrast similarly.

FIG 8. *sigB*, *yjbI*, *and yjbH* mutant phenotypes in response to stress. Serial dilutions of WT, *yjbH*, *sigB* (JMB2745), and *yjbH sigB* mutants were exposed to either **(A)** 1 mM 2,2-dipyridyl or **(B)** 25 mM methyl viologen. Pictures are representative of multiple experiments and include positive controls (+con) of *fhuA* or *sodM* for panels A and B, respectively. **(C)** Aconitase activity under high aeration in *yjbI* and *yjbH* mutants with and without *sigB*. Data is the average (n = 3) with SD. *, $p < 0.01$ compared to WT and "ns" indicates no significant difference by one-way ANOVA with Tukey's multiple comparison test.

FIG 9. Relationship of the *yjbIH* phenotypes to Spx and σ^B. **(A)** Colony pigment of strains grown overnight on TSA plates. **(B)** Aur activity assay using 1% skim milk agar plate.

FIG 10. The *yjbIH* mutant strain shows increased virulence in a murine sepsis model. **(A)** For the low dose, mice were infected with $4x10^6$ CFU of WT (n = 4) or *yjbIH* (n = 5) strains. **(B)** For the high dose, mice were infected with $1x10^7$ CFU of WT (n = 14) or *yjbIH* (n = 13) strains. For percent weight loss, area under the curve (AUC) was calculated for WT (n = 12) and *yjbIH* (n = 11) strains. One mutant-infected mouse

succumbed to infection on day 5 and is excluded from the analysis. Error bars represent SD. * $p \leq 0.01$ as determined by the Mann-Whitney test. **(C)** Mice were infected with $1x10^7$ CFU of either WT, *yjbIH*, *yjbIH* complement, *yjbI*, or *yjbH* strains. For panel C, *n* = 10, but 3 WT-, 2 *yjbIH*-, and 3 *yjbIH* complement-infected mice were at or below the level of detection (LOD; = 100 CFU/mL) and symbols are not shown, but were included in the analysis.

FIG 11. Model of YjbIH, Spx, and σ^B interactions. **(A)** Known interactions of YjbH, Spx, ClpXP, and RNAP. **(B)** Model to account for Aur and pigment phenotypes described here. Briefly, Spx and σ^B both regulate the production of *aur* and *crt*, but σ^B is a stronger regulator of both (denoted by thicker lines), making the *sigB* mutant phenotype dominant over an *spx* mutant. In this model, the absence of YjbH leads to increased levels of Spx which suppresses the expression of *aur* and *crtOPQMN*. In the absence of *sigB* alone, Aur increases and *crtOPQMN* decreases. But in the absence of YjbH and σ^B, Spx increases to shut down *aur* expression. This model accounts for the *sigB* mutant phenotypes being dominant over the *spx* mutation and how the *sigB* mutation can be dominant over the *yjbH* mutation in pigment but not Aur activity. However, this model is likely simplistic and it is not yet known whether Spx works directly through σ^B in some phenotypes, if other regulators are involved, or if YjbH interacts or influences other systems, which is likely.

TABLE 1: Strains and plasmids used in this study.

Strain or plasmid	Description*	Reference
Strains		
AH1263	USA300 CA-MRSA strain LAC lacking LAC-p03, wild-type strain used for these studies	(104)
AH1358	AH1263 Δ*aur*	A. Horswill
CB1400	8325-4 *spx*::*kan*^{R} *geh*::pCL25 *spx*$^+$ *tet*^{R}	(64)
Escherichia coli DH5α	F$^-$Φ80*dlacZ*Δ*M*15 Δ(*lacZYA-argF U169 deoR supE44 hsdR17 recA1 endA1 gyrA96 thi-1 relA1*)	(57)
Escherichia coli DH5α λ*pir*	DH5α lysogenized with λ*pir*	(58)
JE2	Parent strain for NΣ mutants	(50)
JLB110	AH1263 Δ*yjbIH*	This study
JLB112	AH1263 *crtM*::NΣ	(105)
JLB126	JE2 *sigB*::*kan*^{R}	This study
JLB130	AH1263 *sigB*::NΣ	(105)
JLB134	AH1263 Δ*yjbI*	This study
JLB143	JLB110 *sigB*::NΣ	This study
JLB144	AH1263 *0904*::NΣ	This study
JLB146	AH1263 *hmp*::NΣ	This study
JLB147	AH1263 Δ*yjbH*	This study
JLB174	AH1263 *sigB*::*kan*^{R}	This study
JLB175	AH1263 Δ*yjbIH sigB*::*kan*^{R}	This study
JLB176	AH1263 *clpP*::NΣ	This study
JLB178	JLB110 *clpP*::NΣ	This study
JLB179	JLB110 *crtM*::NΣ	This study
JLB247	JLB110 *geh*::pCL25 *spx*$^+$ *tet*^{R}	This study

JLB248	AH1263 pMK4-pGlyS-*trxA spx*::*kan*^{R}	This study
JLB249	AH1263 pMK4-pGlyS-*trxA spx*::*kan*^{R} *0904*::NΣ	This study
JLB250	AH1263 pMK4-pGlyS-*trxA spx*::*kan*^{R} *0904*::NΣ *geh*::pCL25 *spx*$^+$ *tet*^{R}	This study
JLB264	AH1263 *sigB*::*tet*^{R}	This study
JLB277	AH1263 pMK4-pGlyS-*trxA spx*::*kan sigB*::*tet*	This study
JLB278	AH1263 Δ*yjbIH attC*::*yjbIH***	This study
JLB279	AH1263 Δ*yjbH attC*::*yjbH***	This study
JLB280	AH1263 pMK4-pGlyS-*trxA spx*::*kan 0904::NΣ sigB*::*tet*	This study
JMB2078	AH1263 *katA*::*erm*^{R} (SAUSA300_1232)	(87)
JMB2745	AH1263 *sigB*::NΣ (SAUSA300_1109)	This study
JMB5853	AH1263 *sodM*::NΣ	(87)
JMB7525	AH1263 *fhuA*::NΣ	(86)
JMB7924	AH1263 *acnA*::*tet*^{R} pEPSA5_*acnA*	(75, 87)
JMB8838	AH1263 Δ*yjbI acnA*::*tet*^{R} pEPSA5_*acnA*	This study
JMB8840	AH1263 Δ*yjbIH acnA*::*tet*^{R} pEPSA5_*acnA*	This study
JMB8849	AH1263 Δ*yjbH acnA*::*tet*^{R} pEPSA5_*acnA*	This study
JMB8972	AH1263 Δ*yjbH sigB*::NΣ	This study
JMB8974	AH1263 Δ*yjbI sigB*::NΣ	This study
MV58	*Escherichia coli K12* DH5α with pMK4-pGlyS-*trxA*	(64)
NE406	Strain containing *fhuA*::NΣ (SAUSA300_0633)	(50)
NE896	Strain containing *yjbH*::NΣ (SAUSA300_0903)	(50)
NE912	Strain containing *clpP*::NΣ (SAUSA300_0752)	(50)
NE1109	Strain containing *sigB*::NΣ (SAUSA300_2022)	(50)

NE1444	Strain containing *crtM*::NΣ (SAUSA300_2499)	(50)
NE1744	Strain containing *hmp*::NΣ (SAUSA300_0234)	(50)
NE1800	Strain containing *yjbI*::NΣ (SAUSA300_0904)	(50)
NE1932	Strain containing *sodM*::NΣ (SAUSA300_1513)	(50)
RN4220	Highly transformable *S. aureus*	(60)
Plasmids		
pCK3	P_{aur} – *lacZ* reporter plasmid; Amp^R, Cm^R	This study
pCM28	*E. coli-S. aureus* shuttle vector; Amp^R, Cm^R	(106)
pCP1	Δ*yjbI* allelic exchange plasmid; Amp^R, Cm^R	This study
pCP2	Downstream *yjbH* cloned into pJB38	This study
pCP3	Δ*yjbH* allelic exchange plasmid; Amp^R, Cm^R	This study
pCP4	*yjbIH* complementation plasmid; Trm^R	This study
pCP5	*yjbH* complementation plasmid; Trm^R	This study
pCP6	*yjbI* complementation plasmid; Trm^R	This study
pCP7	P_{crtM} – *lacZ* reporter plasmid; Amp^R, Cm^R	This study
pEPSA5 *acnA* (p*acnA*)	*acnA* cloned under a xylose-inducible promoter	(75)
pJB38	Temperature-sensitive allelic exchange plasmid	(59)
pJB158	pCM28-based *yjbIH* complement plasmid	This study
pJB185	Promoterless codon-optimized *lacZ*; Amp^R, Cm^R	(68)
pJB1021	Δ*yjbIH* allelic exchange plasmid; Amp^R, Cm^R	This study
pKAN	NE1109 kanamycin exchange plasmid	(59)
pKK22	Stable *in vivo* plasmid	(65)
pMK4-pGlyS-*trxA*	*trxA* cloned under the *glyS* promoter into the pMK4 vector	(64)
pTET	NE1109 tetracycline exchange plasmid	(59)

*NΣ, bursa aurealis transposon insertion; Amp^R, ampicillin resistance in *E. coli*; Cm^R, chloramphenicol resistance in *S. aureus*; Trm^R, trimethoprim in *E. coli* and *S. aureus*; Kan^R, kanamycin in *S. aureus*; Erm^R, in *S. aureus*; Tet^R, tetracycline resistance in *S. aureus*.

**Integrated into the chromosomal attachment site (*attC*) in *S. aureus* pathogenicity island 1 (SapI1).

1094 **TABLE 2: Oligonucleotides used in this study.**

Name	Sequence (5' – 3')*	Purpose
Asp23F	CGCTGCACGTGAAGTTAAAG	*asp23* qPCR – forward
Asp23R	GCAGCTTGTTTTTCACCAAC	*asp23* qPCR – reverse
CNK11	ccgGAATTCGGCATATTAAGGCTAGAGTGTGAGG	Amplification of *aur* promoter to clone into pCK3
CNK12	gcTCTAGAAGTGCTCAACAAGGTTAATGCTGC	Amplification of *aur* promoter to clone into pCK3
CP1	caGGTACCCAGAGATGAACTTGATTATTTCAAACGAC	Amplification of *yjbH* upstream
CP2	ccggctagCGAGTCAGTAAAAAGACCTCGTTACATTTATG	Construction of pCP4 complementation plasmid and *yjbIH* RT-PCR
CP3	gccggatccAGAGATGAACTTGATTATTTCAAACGAC	Construction of pCP6 complementation plasmid
CP7	ccgcctaggGAGTCAGTAAAAAGACCTCGTTACATTTATG	Construction of pCP5 complementation plasmid
CP8	ccgcctaggGAATTATTATGTATATCAATACGCAACTG	Construction of pCP6 complementation plasmid
CP9	gcagGAATTCCTCGTACAATTTCAGCAAACCAAGC	Amplification of *crtM* promoter to clone into pCP7
CP10	ggcGTCGACCATCTAAATTGAATCACTCTCAATCATAC	Amplification of *crtM* promoter to clone into pCP7
CP27	AACCATTAACAGCGCCATTT	*trxB* qPCR – forward
CP28	AACCTTTGTCGCGAACATCT	*trxB* qPCR – reverse

CP29	CCAACTGATGGATACGGCTA	*katA* qPCR – forward
CP30	CCATTGCATTTGCTGTATTTG	*katA* qPCR – reverse
CP73	TTCTGAATGTGGATGGCCTA	*msrAB* qPCR – forward
CP74	TGAACGCACTTCAGTTCTCA	*msrAB* qPCR – reverse
CP75	TCAGGTTGGGCTTGGTTAGT	*sodA* qPCR – forward
CP76	TAAGCGTGTTCCCATACGTC	*sodA* qPCR – reverse
CP77	CAGTGGGGCACTTTAGAT	*sodM* qPCR – forward
CP78	TTGGCGTTGTCACAATTTCT	*sodM* qPCR – reverse
CP79	ATTATCGACCCAGACGGTGT	*ahpC* qPCR – forward
CP80	GCCAGGGTTTTTACGAACAT	*ahpC* qPCR – reverse
CP85	AGCACTTTCACCTGATTTTCC	*perR* qPCR – forward
CP86	GAATCGACTTGATGAGTCTCCA	*perR* qPCR – reverse
CP91	GCCTCTGCCAAAGGTTTAGA	*hmp* qPCR – forward
CP92	GTCATGATGGCTTGCGATAC	*hmp* qPCR – reverse
JBKU19	ccGGTACCGAGGTGTATACATATCATGGCAACAAATC	Amplification of *yjbI* upstream
JBKU20	ccgctagcCATTTAATCACCCATTTTCAAAAATTTACTG	Amplification of *yjbI* upstream
JBKU23	ccgctagcCCTAAAATCAAATCAAAATAAATAAATTAAAG	Amplification of *yjbH* downstream
JBKU24	ccgtcgacGAATTATTATGTATATCAATACGCAACTG	Amplification of *yjbH* downstream
JBKU42	gccGCTAGCCATGTTTATTCACCTACAATTAATTTTAGG	Amplification of *yjbH* upstream
JBKU43	ccGCTAGCTAAAATTAATTGTAGGTGAATAAACATGGC	Amplification of *yjbI* downstream
JBKU44	gagcGTCGACTTCCATCGTTACAAGTTGTTGTTGC	Amplification of *yjbI*

		downstream
JBPR01	ccggatcCACCAGCAAAGGTTGGTCTATTAGAATAC	Construction of pCP4, pCP5, and pJB158 complementation plasmids
JBPR02	ggctgcaGACCTCGTTACATTTATGGTGTACGAGGTC	Construction of pJB158 complementation plasmid
JBPR03	ATGACAACAACACCATATGACATCATTGGTAAAG	*yjbIH* RT-PCR
JBSIGAF	AACTGAATCCAAGTGATCTTAGTG	qPCR - *sigA* internal control forward
JBSIGAR	TCATCACCTTGTTCAATACGTTTG	qPCR - *sigA* internal control reverse

*Upper case letters denote *S. aureus*-derived sequences; underlined regions are restriction enzyme sites; lower case letters are non-homologous bases added for cloning purposes. All primers originate from this study.

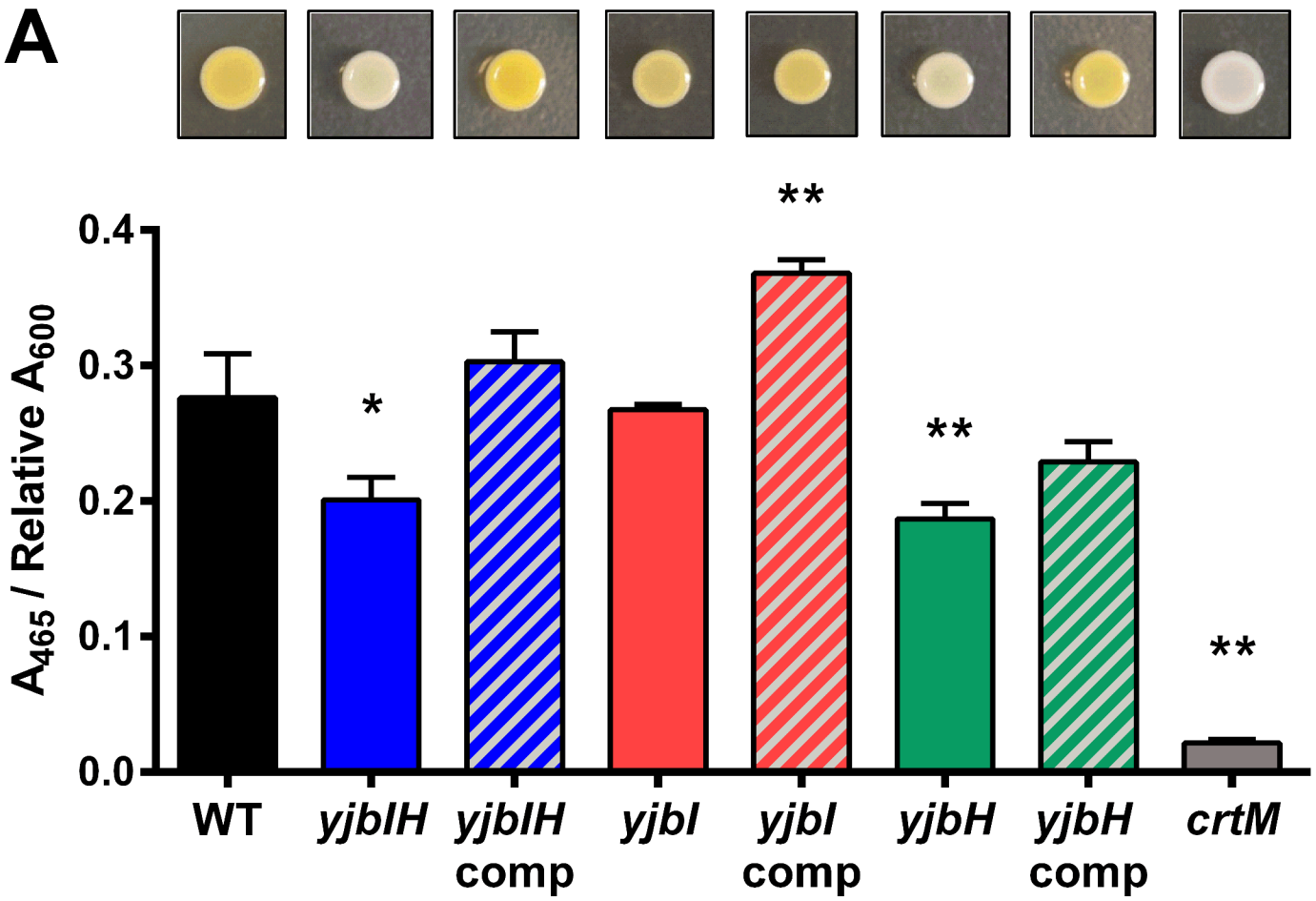
A
0.4
0.3
0.2
0.1
0.0
A_{465} / Relative A_{600}
*
**
**
**
WT
yjblH
yjblH comp
yjbI
yjbI comp
yjbH
yjbH comp
crtM
B
WT
aur
yjblH
yjblH comp
yjbI
yjbI comp
yjbH
yjbH comp

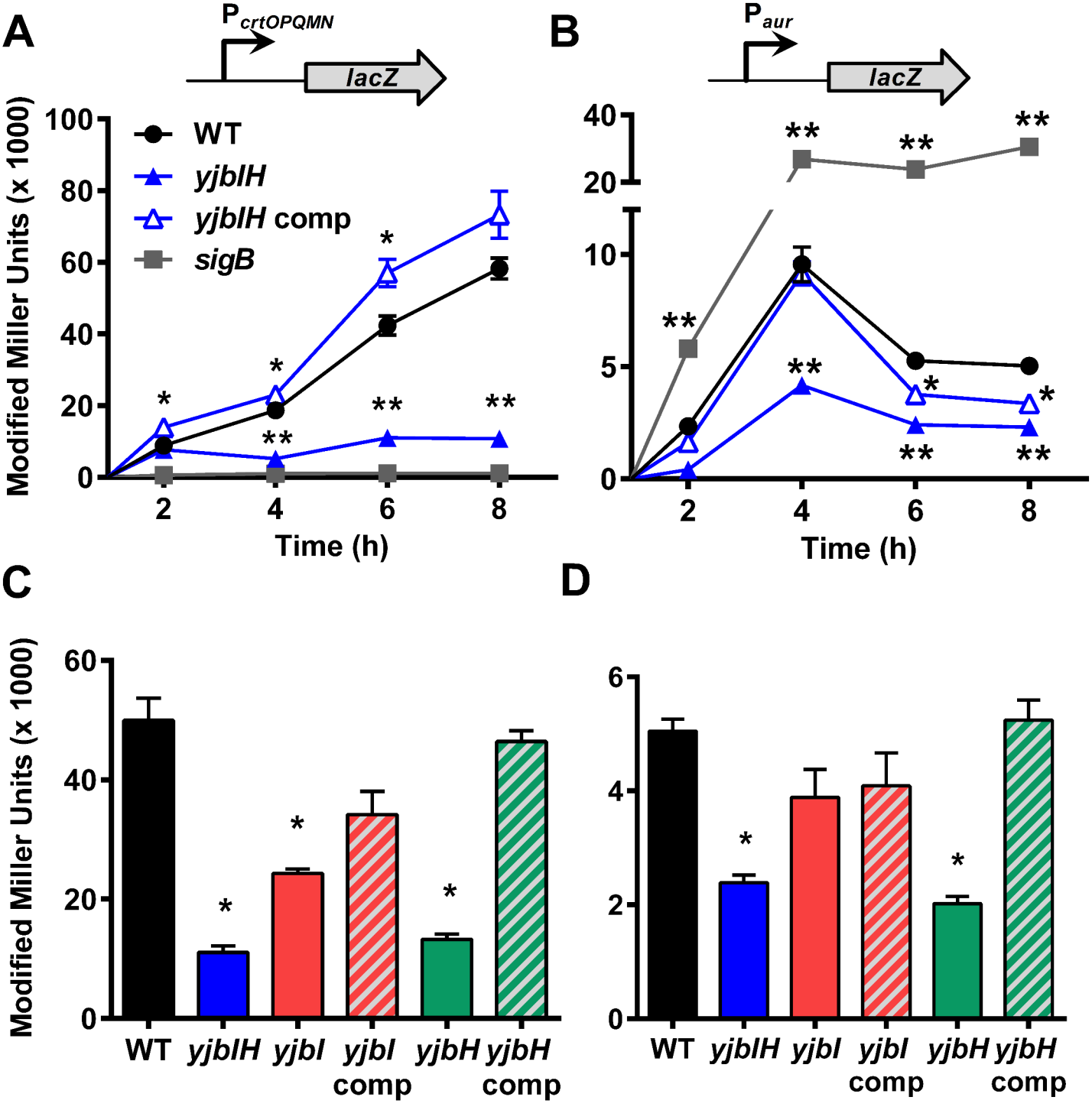
A
P crtOPQMN
lacZ
Modified Miller Units (x 1000)
WT
yjblH
yjblH comp
sigB
Time (h)
B
P aur
lacZ
Time (h)
C
Modified Miller Units (x 1000)
WT
yjblH
yjbI
yjbI comp
yjbH
yjbH comp
D
WT
yjblH
yjbI
yjbI comp
yjbH
yjbH comp

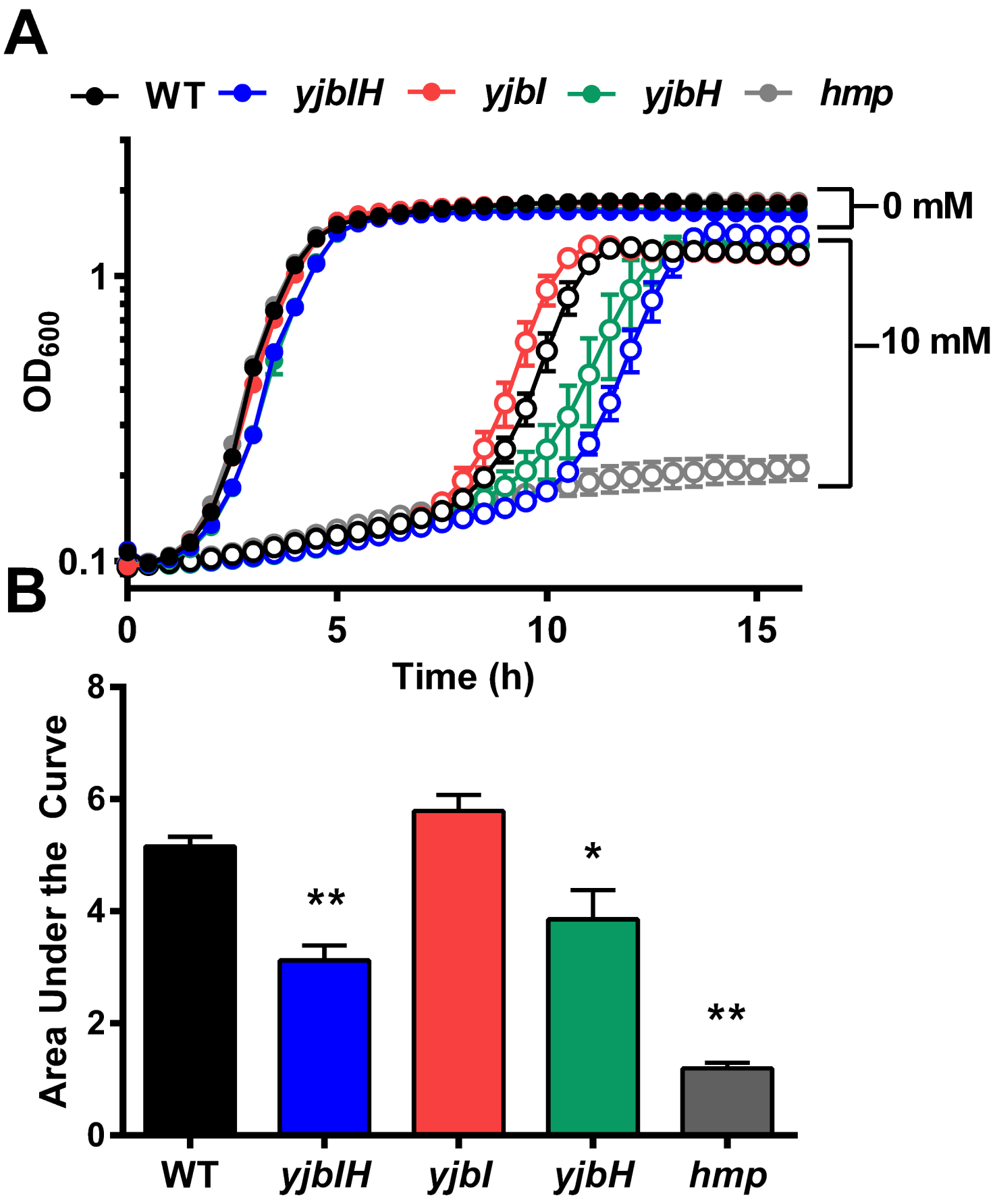
A
WT
yjblH
yjbl
yjbH
hmp
0 mM
10 mM
OD600
1
0.1
0
5
10
15
Time (h)
B
Area Under the Curve
8
6
4
2
0
**
*
**
WT
yjblH
yjbl
yjbH
hmp

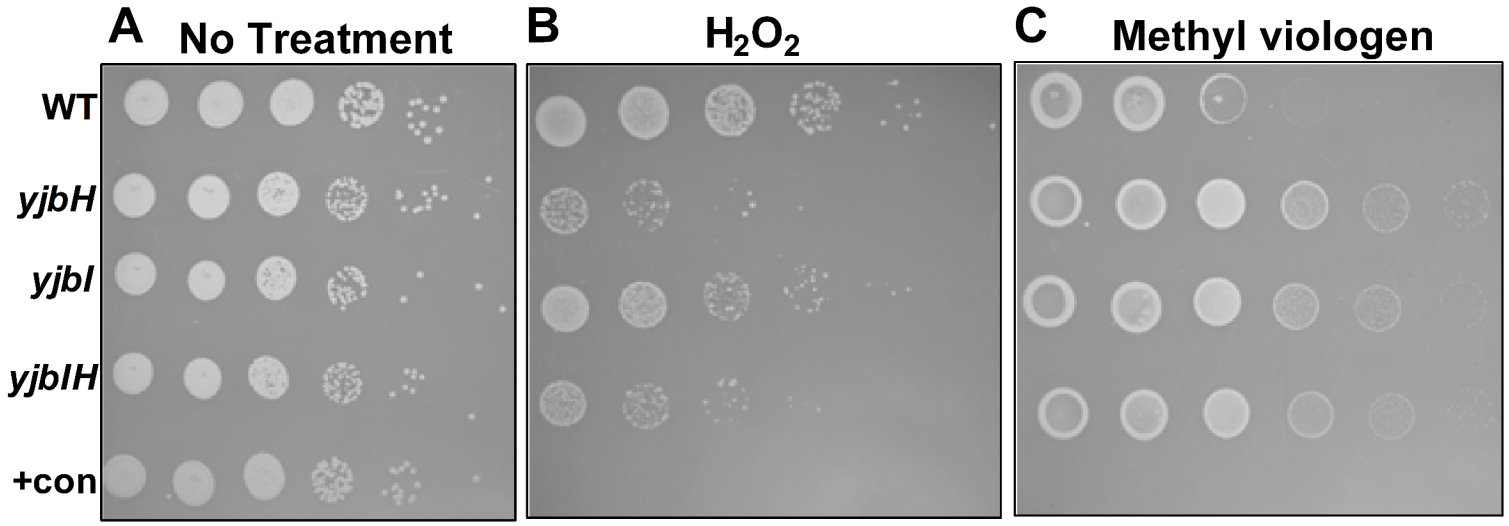
A
No Treatment
B
H_2O_2
C
Methyl viologen
WT
yjbH
yjbI
yjbIH
+con

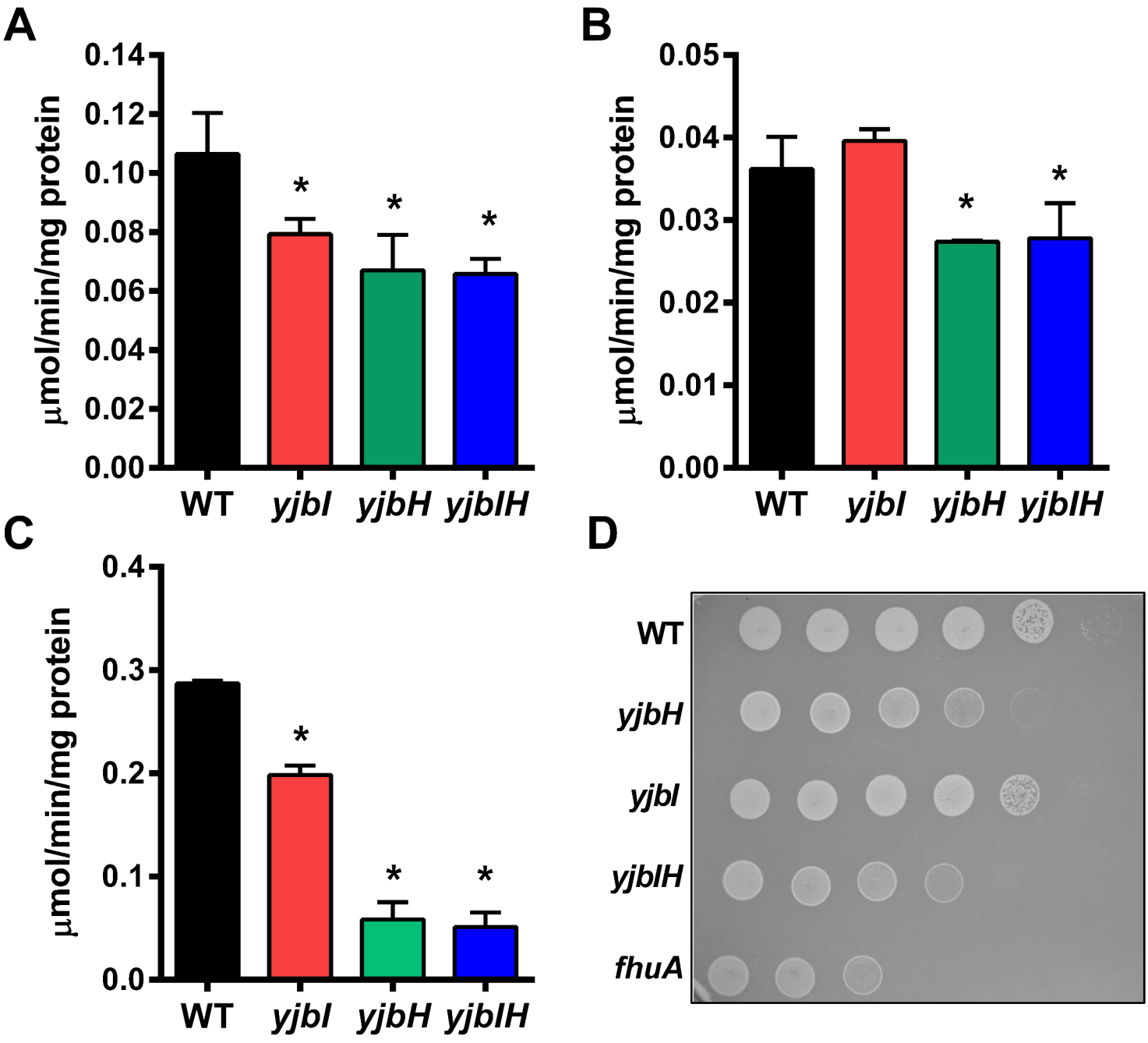
A
0.14
0.12
0.10
0.08
0.06
0.04
0.02
0.00
µmol/min/mg protein
*
*
*
WT
yjbI
yjbH
yjbIH
B
0.05
0.04
0.03
0.02
0.01
0.00
µmol/min/mg protein
*
*
WT
yjbI
yjbH
yjbIH
C
0.4
0.3
0.2
0.1
0.0
µmol/min/mg protein
*
*
*
WT
yjbI
yjbH
yjbIH
D
WT
yjbH
yjbI
yjbIH
fhuA

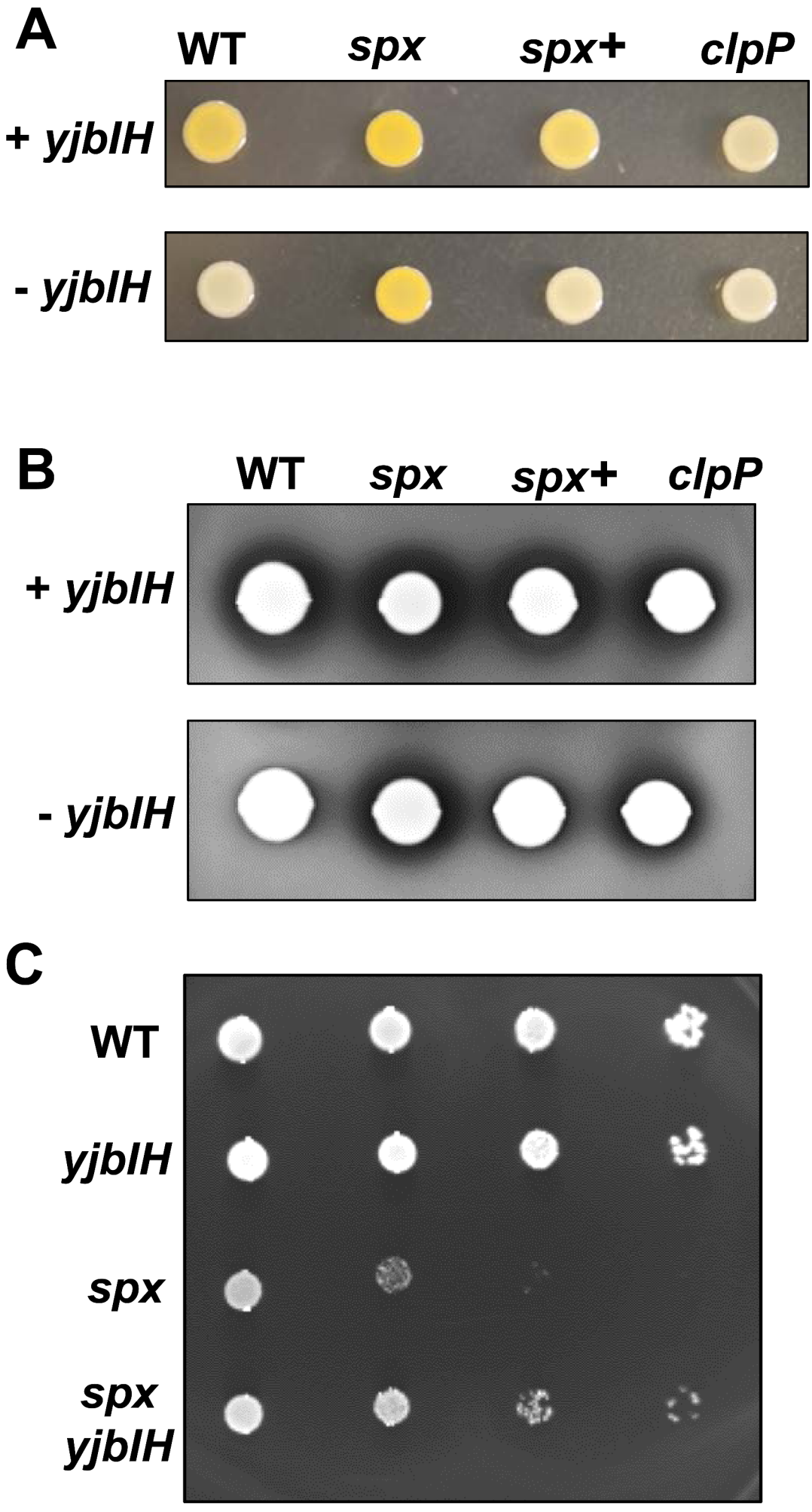
A
WT
spx
spx+
clpP
+ yjblH
- yjblH
B
WT
spx
spx+
clpP
+ yjblH
- yjblH
C
WT
yjblH
spx
spx
yjblH

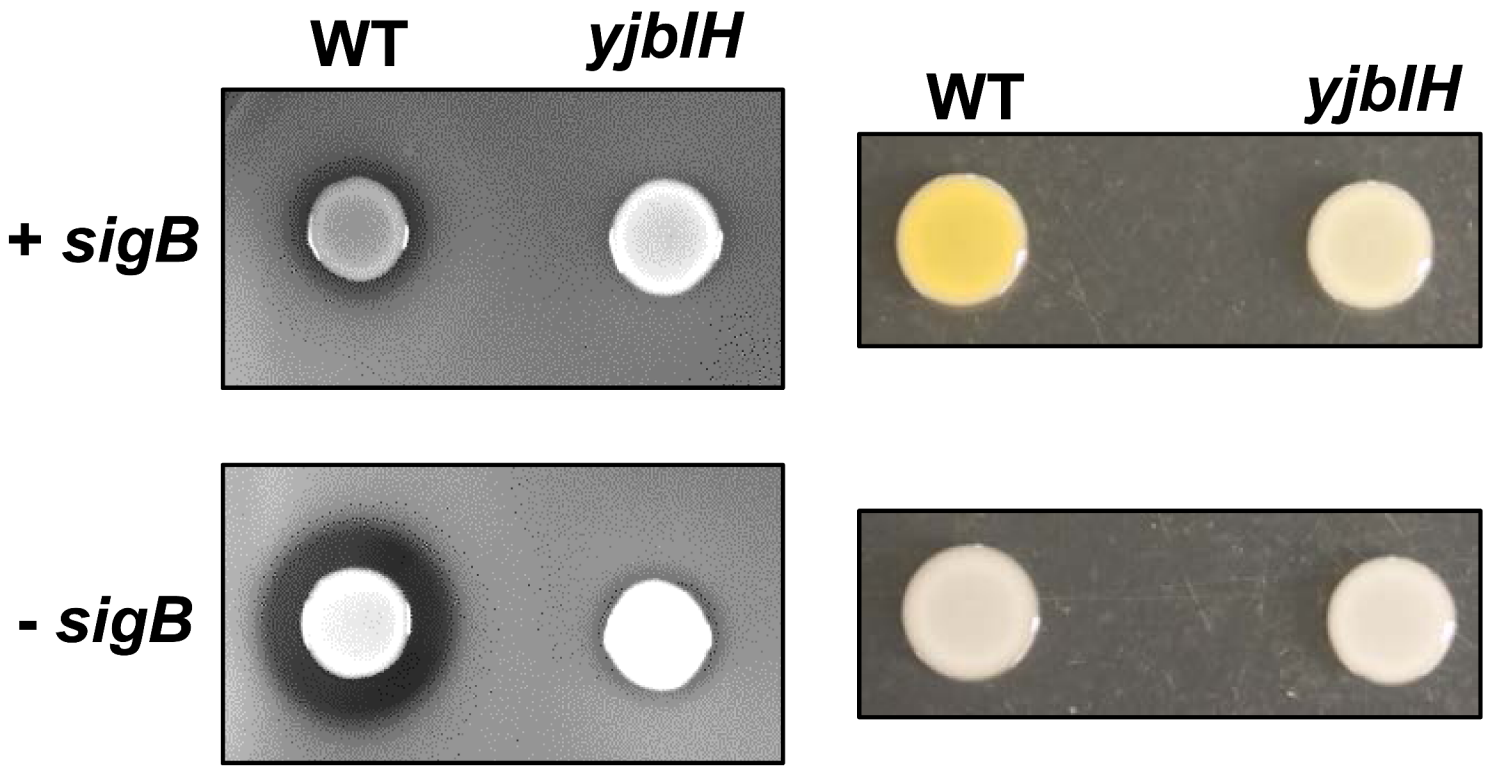
WT
yjbIH
WT
yjbIH
+ sigB
- sigB

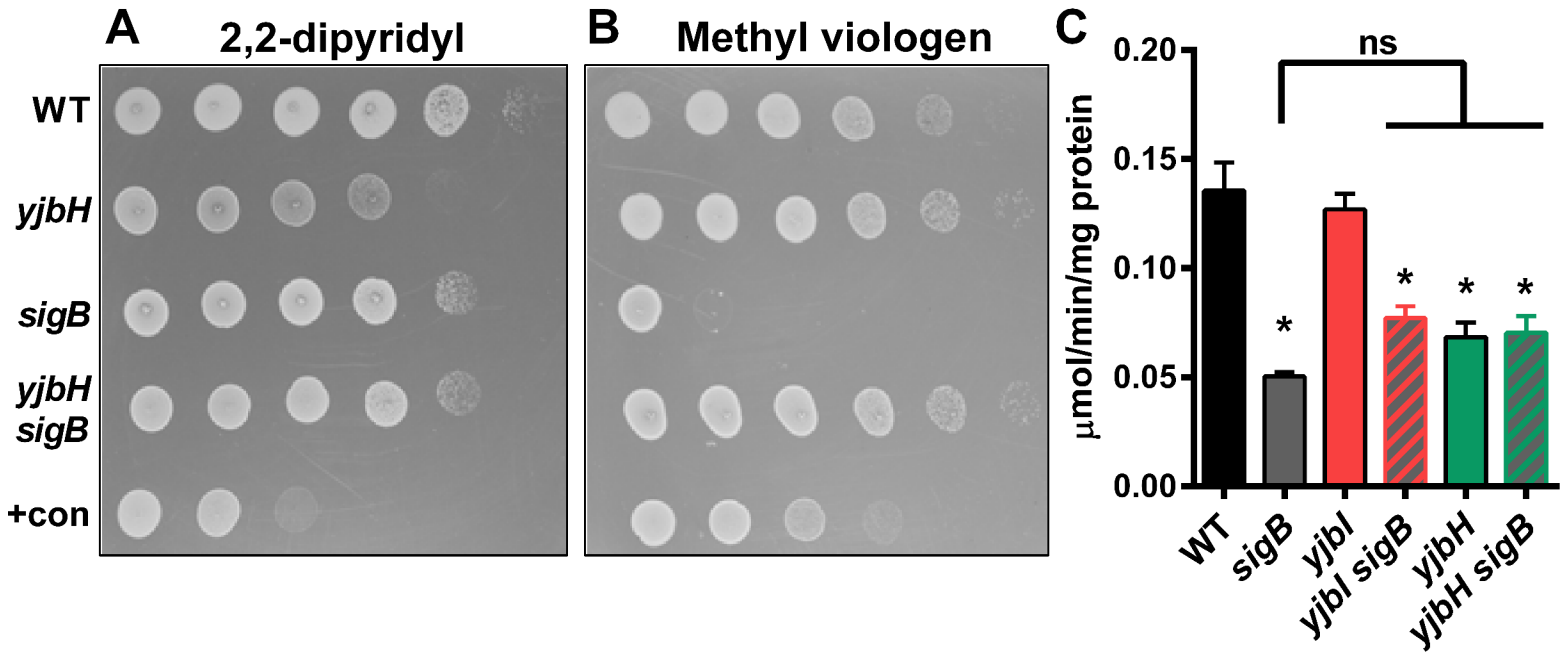
A
2,2-dipyridyl
B
Methyl viologen
C
WT
yjbH
sigB
yjbH sigB
+con
ns
0.20
0.15
0.10
0.05
0.00
µmol/min/mg protein
*
*
*
*
WT
sigB
yjbI
yjbI sigB
yjbH
yjbH sigB

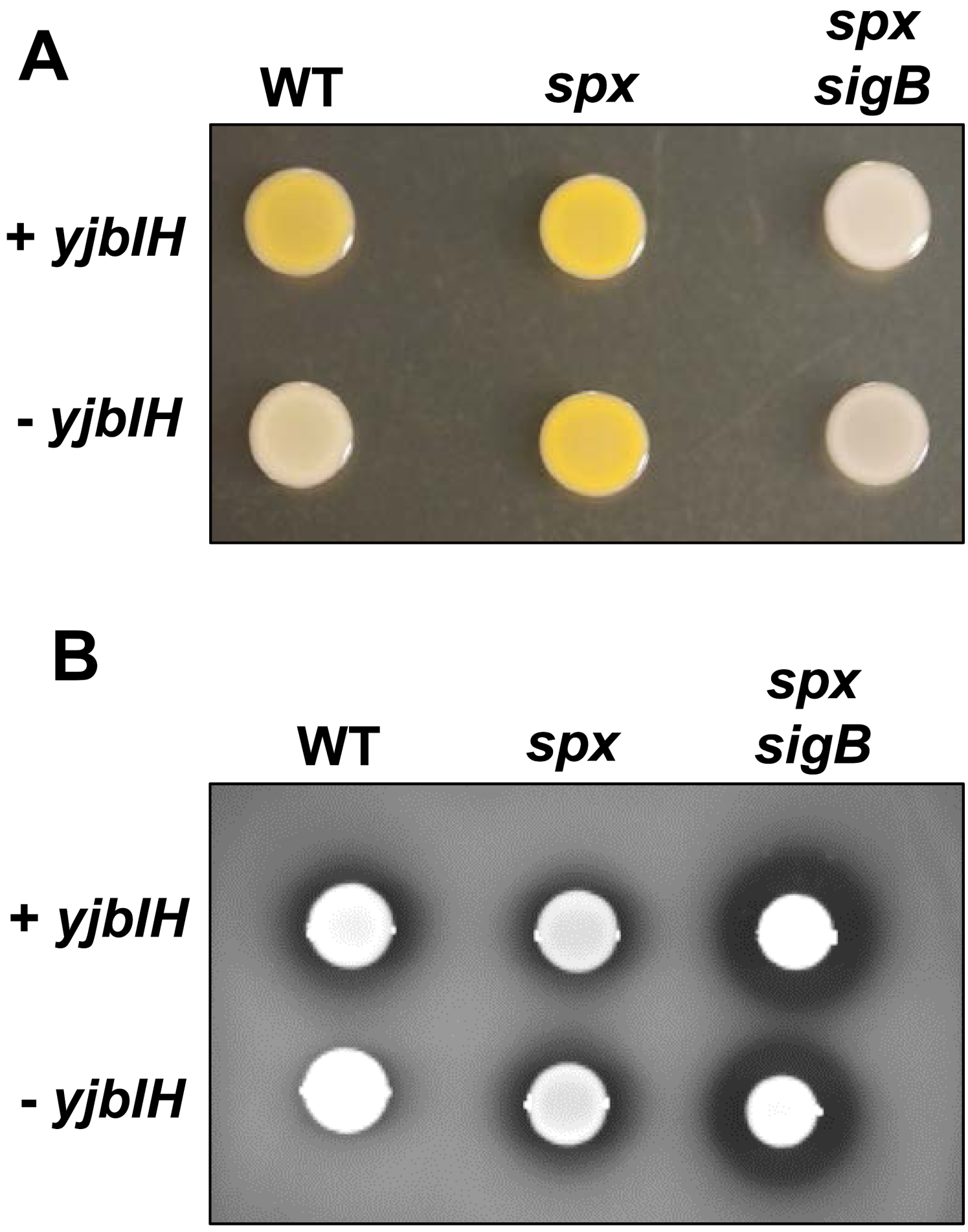
A
WT
spx
spx sigB
+ yjbIH
- yjbIH
B
WT
spx
spx sigB
+ yjbIH
- yjbIH

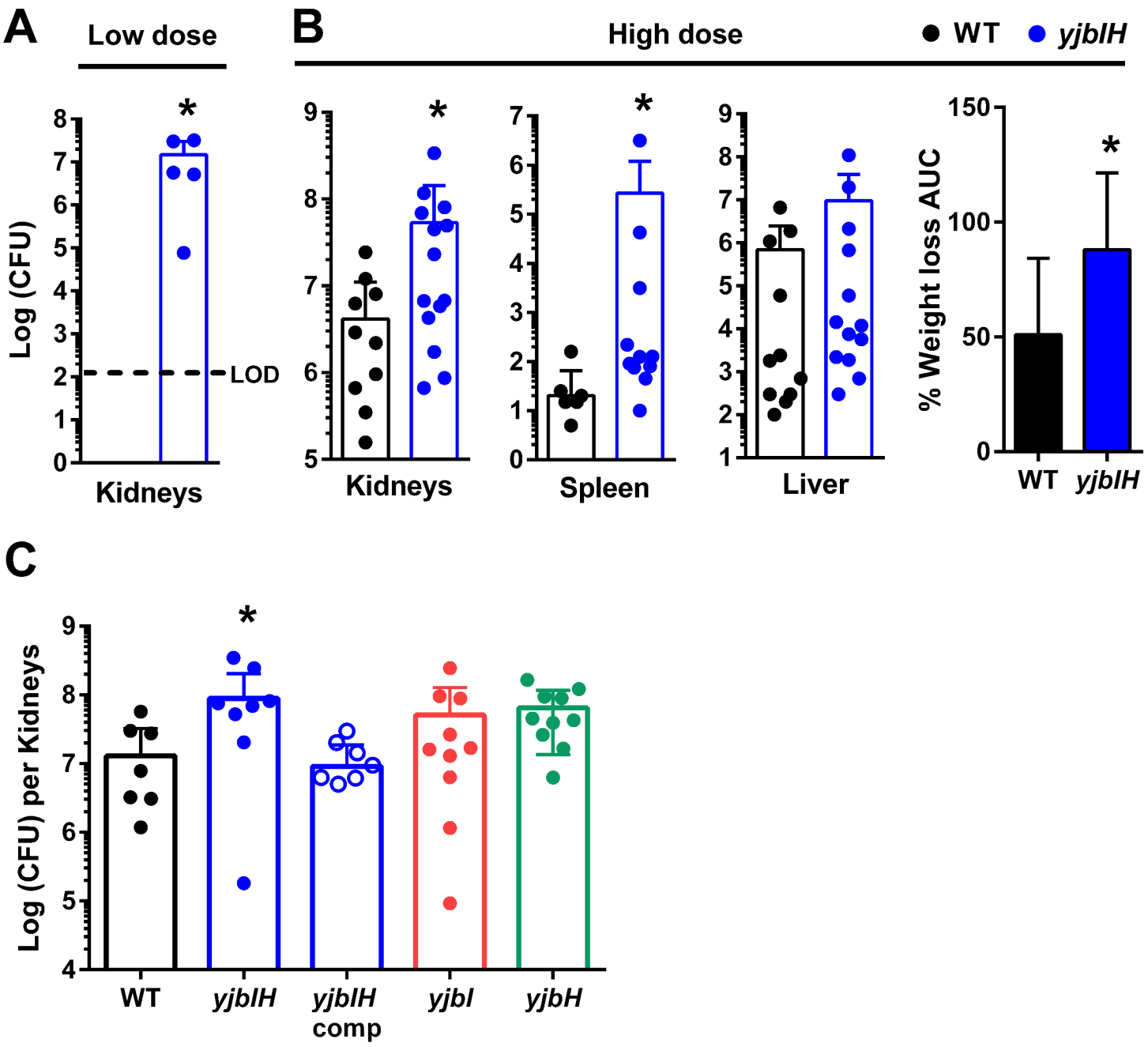
A
Low dose
B
High dose
WT
yjblH
Log (CFU)
LOD
Kidneys
Kidneys
Spleen
Liver
% Weight loss AUC
WT
yjblH
C
Log (CFU) per Kidneys
WT
yjblH
yjblH comp
yjbI
yjbH

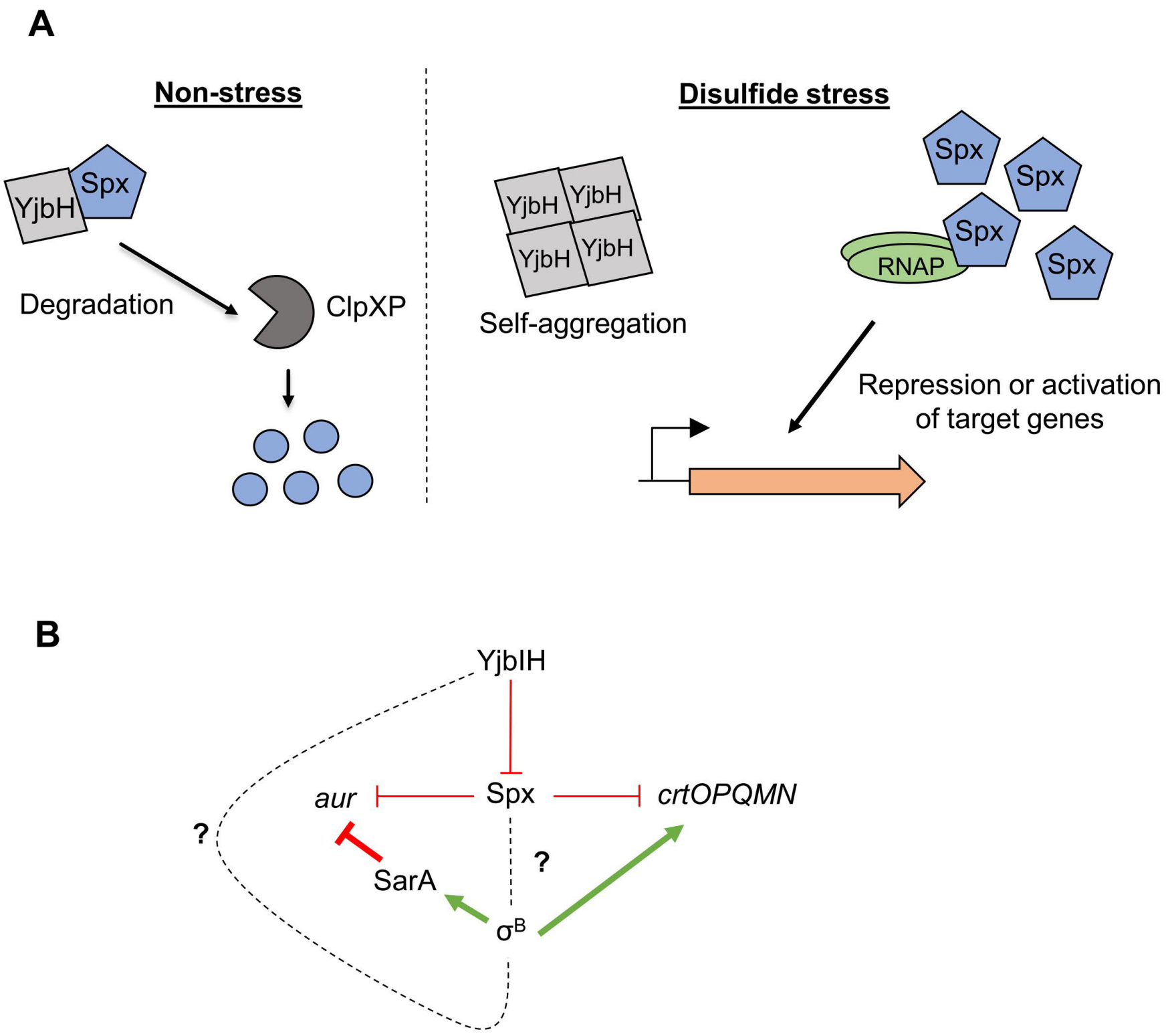
A
Non-stress
YjbH
Spx
Degradation
ClpXP
Disulfide stress
YjbH
YjbH
YjbH
YjbH
Self-aggregation
Spx
Spx
Spx
RNAP
Spx
Repression or activation
of target genes
B
YjbIH
aur
Spx
crtOPQMN
?
SarA
?
σB